



FEATURE ARTICLE

# An open spatial capture–recapture framework for estimating the abundance and seasonal dynamics of white sharks at aggregation sites

Megan V. Winton<sup>1,2,\*</sup>, Gavin Fay<sup>2</sup>, Gregory B. Skomal<sup>3</sup>

<sup>1</sup>Atlantic White Shark Conservancy, North Chatham, MA 02650, USA

<sup>2</sup>Department of Fisheries Oceanography, School for Marine Science and Technology, University of Massachusetts Dartmouth, New Bedford, MA 02744, USA

<sup>3</sup>Massachusetts Division of Marine Fisheries, New Bedford, MA 02744, USA

**ABSTRACT:** The present study provides the first estimate of abundance for the white shark at a new aggregation site in the western North Atlantic, which required the development of a novel modeling framework to accommodate the species' migratory behavior. Estimates of abundance are needed to evaluate the performance of existing conservation measures for white shark populations worldwide but have historically been infeasible to obtain in the region. Following the recent emergence of Cape Cod, Massachusetts, USA, as a seasonal aggregation site, we conducted a photographic capture–recapture survey and identified 393 individual white sharks from 2015–2018. As conventional capture–recapture models do not adequately represent the species' migratory behavior, we extended an existing open spatial capture–recapture framework to allow for movements into and out of the surveyed area and accommodate variation in residency and habitat use among individuals. Using simulations, we demonstrated that failing to account for these processes resulted in biased estimates of abundance that would be misleading if used as the basis for management advice. We applied the model developed to describe the seasonal dynamics of the Cape Cod aggregation site and estimated a superpopulation size of 800 (393–1286) individuals, which provides an important baseline for this species of conservation concern. Because it directly links changes in abundance over time to the demographic processes underpinning them, the model described provides a more mechanistic understanding of the dynamics of white shark aggregations and improves the applied relevance of the results for the conservation and management of the species.



A white shark investigates the camera during a photographic capture–recapture survey conducted off Cape Cod, Massachusetts, USA.

*Photo: Massachusetts Division of Marine Fisheries, Research Supported by Atlantic White Shark Conservancy*

**KEY WORDS:** Open population mark–recapture · *Carcharodon carcharias* · Photographic identification · Western North Atlantic · Telemetry-integrated model · Highly migratory species

## 1. INTRODUCTION

Global concern about the conservation status of the white shark *Carcharodon carcharias* has afforded the species a relatively high degree of national and international protection, but the status of many popula-

\*Corresponding author: megan.winton@gmail.com

tions remains unknown (Huveneers et al. 2018). One of the largest (reaching lengths of up to 6 m; Castro 2012) and most feared shark species, the white shark is long-lived, slow-growing, late to mature, and consequently highly vulnerable to overexploitation (Natanson & Skomal 2015). Although the species was never the target of large-scale directed fisheries, white shark populations throughout its circumglobal range declined as commercial and recreational fisheries and shark control programs expanded during the latter half of the twentieth century (Roff et al. 2018). In some regions, it is estimated that white shark abundance decreased by as much as 70–90% (McPherson & Myers 2009, Reid et al. 2011, Curtis et al. 2014, Roff et al. 2018) before protections began to be put into place in the 1990s by both individual countries and international treaties (United Nations Convention on the Law of the Sea Annex I, Convention of International Trade in Endangered Species of Wild Fauna and Flora Appendix II, Convention on the Conservation of Migratory Species of Wild Animals Appendix I and II). Following the implementation of protective legislation, white shark populations in several regions have shown signs of recovery (Lowe et al. 2012, Curtis et al. 2014). However, estimates of abundance, which are needed to evaluate the performance of existing conservation measures and aid in future management decisions, remain unavailable for many populations (Huveneers et al. 2018).

Efforts to estimate white shark abundance in the western North Atlantic (WNA) have proven particularly challenging. Despite the white shark's long and storied history in the region (Gudger 1950, Casey & Pratt 1985, Mollomo 1998), it was until recently considered an elusive species whose migratory habits and low natural abundance as an apex predator rendered it so sparsely distributed that 'any attempt to estimate ... abundance can only be expressed in general terms' (Casey & Pratt 1985, p. 6). Trends in catch records indicate substantial population declines prior to the establishment of a fishery management plan that enacted commercial and recreational regulations for large coastal shark species in the US Atlantic in 1993 and the subsequent prohibition of the harvest of white sharks in 1997 (Curtis et al. 2014). In the early 2000s, the number of reported white shark sightings began to increase, particularly along the eastern coastline of Cape Cod, Massachusetts (Skomal et al. 2012). This increase has largely been attributed to the local population recovery of gray seals *Halichoerus grypus* following the 1972 passage of the Marine Mammal Protection Act (Skomal et al.

2012) but also likely reflects the preliminary recovery of the white shark population itself (Curtis et al. 2014). During the summer and fall months, white sharks hunt for locally abundant pinniped prey along the Cape Cod shoreline and are now accessible to targeted research efforts for the first time in the WNA (Winton et al. 2021). The emergence (or more likely re-emergence; Skomal et al. 2012) of Cape Cod as a seasonal aggregation site has provided a unique opportunity to apply capture–recapture methods to generate the first robust estimate of white shark abundance in any portion of its WNA range.

Capture–recapture studies are widely used to estimate the size of wildlife populations and have been conducted in other areas where white sharks aggregate (Cliff et al. 1996, Strong et al. 1996, Chapple et al. 2011, Sosa-Nishizaki et al. 2012, Towner et al. 2013, Andreotti et al. 2016, Becerril-García et al. 2020). These approaches are based on reconstructing encounter histories over time and require that individuals are 'marked' in some way that makes them distinguishable from other individuals in the population. Early white shark capture–recapture surveys used conventional fisheries dart tags to mark individuals (Cliff et al. 1996, Strong et al. 1996), but the realization that individual sharks could be identified by their unique coloration and dorsal fin profiles revolutionized researchers' ability to efficiently and non-invasively obtain encounter history data (Klimley & Anderson 1996, Strong et al. 1996, Domeier & Nasby-Lucas 2007). Photographic identification (hereafter photo-ID) surveys have been used to monitor and estimate the size of white shark aggregations in the eastern North Pacific and Indian oceans (Chapple et al. 2011, Sosa-Nishizaki et al. 2012, Towner et al. 2013, Andreotti et al. 2016), but the appropriateness of the analytical approaches used to do so has become the subject of some debate.

Criticism of analytical approaches has centered on concerns that the models applied to estimate abundance do not adequately represent the complex processes generating the observed encounter histories (Burgess et al. 2014, Irion et al. 2017). Conventional capture–recapture models were developed for closed populations (i.e. no individuals are born, die, enter, or leave the area) and assume that all individuals have a constant and equal probability of encounter during survey periods (Otis et al. 1978). These are problematic constraints for species that are highly migratory, such as the white shark. Individual white sharks travel thousands of kilometers each year to optimize foraging opportunities but are only available to survey efforts at coastal aggregation sites that

constitute a small fraction of their overall range (Domeier & Nasby-Lucas 2013, Skomal et al. 2017). Although many white sharks exhibit long-term fidelity to aggregation sites (Anderson et al. 2011), short-term patterns of space use and residency at such sites vary widely among individuals, and not all individuals visit aggregation sites every year (Domeier & Nasby-Lucas 2013, Skomal et al. 2017). Therefore, individual sharks have variable degrees of exposure to sampling as a function of their location relative to survey efforts; if ignored, this heterogeneity in encounter probabilities can result in biased population estimates that would be misleading if used as the basis for management advice (Burgess et al. 2014). To address this issue, recent estimates of white shark abundance from photo-ID surveys have applied open capture–recapture models that allow individuals to enter and permanently exit the surveyed population and have incorporated variable encounter probabilities among sex and size classes as a proxy for differences in habitat use (Towner et al. 2013, Andreotti et al. 2016, Kanive et al. 2021). However, neither approach fully resolves the problems that have been recognized to date, which are largely a consequence of the lack of spatial context in conventional capture–recapture models.

Spatial capture–recapture (SCR) methods were developed to improve abundance estimates from capture–recapture surveys by formally considering the spatial processes underpinning observed encounter histories. Conceptually, SCR models extend individual-covariate models commonly applied to explain variation in encounter rates among individuals to account for spatial heterogeneity arising from individual differences in space use (Royle et al. 2009). The probability that an individual is encountered is assumed to depend on the distance between the surveyed area and the individual’s center of activity during the survey period; individuals that primarily use habitats outside the surveyed area are less likely to be encountered and vice versa, making the use of SCR models for white sharks intuitively appealing. Furthermore, any type of georeferenced, individual-based data source can be formulated as an SCR model. Therefore, these models also provide a logically consistent basis for directly integrating telemetry data into population models (Royle et al. 2013). Tagging studies are often conducted at aggregation sites in conjunction with capture–recapture surveys, and the results are used indirectly to aid in interpretation of abundance estimates (Burgess et al. 2014). The formal integration of telemetry data into population models has the potential to improve esti-

mates of abundance and other population parameters (Royle et al. 2013, Tenan et al. 2017, Linden et al. 2018), but the application of tag-integrated approaches has been limited, in part because of the lack of available frameworks for incorporating electronic tagging data (Sippel et al. 2015).

In this study, we developed and applied a telemetry-integrated SCR model to estimate white shark abundance from a seasonal photo-ID survey conducted in the nearshore waters along Cape Cod, Massachusetts, from 2015–2018. We extended an existing open SCR framework (Glennie et al. 2019) to allow for movements into and out of the survey area (i.e. temporary emigration; Kendall et al. 1997) and formally integrated tagging data obtained from a concurrent acoustic telemetry array. Using our actual survey design and the proportion of tagged individuals, we conducted simulation testing to determine the impact of accounting for variation in space use, temporary emigration, and integrating acoustic telemetry data on demographic parameter estimates. We applied the resulting model to investigate the seasonal dynamics of the Cape Cod aggregation and generated the first estimate of abundance for white sharks in any portion of their WNA range. This estimate provides a baseline from which the performance of current and future management measures can be assessed for this species of conservation concern.

## 2. MATERIALS AND METHODS

### 2.1. Field sampling

We conducted a seasonal photo-ID survey in the nearshore waters along the Atlantic coast of Cape Cod, known locally as the ‘Outer Cape’ (Fig. 1). Unlike previous capture–recapture surveys of white shark populations (Cliff et al. 1996, Strong et al. 1996, Chapple et al. 2011, Nasby-Lucas & Domeier 2012, Towner et al. 2013, Andreotti et al. 2016), we employed active rather than passive (i.e. attracting sharks with baits) sampling techniques. Sharks were located by an experienced commercial spotter pilot searching Massachusetts state waters (which extend 3 nautical miles from the coast) between the northern and southern tip of Cape Cod, which encompasses an approximately 500 km<sup>2</sup> area (Fig. 1). Prior to the survey trip, the pilot was given a starting direction but was not constrained to a pre-determined flight path in order to maximize encounter rates and survey efficiency. When a shark was spotted, the pilot directed the research vessel to the shark’s location. A video

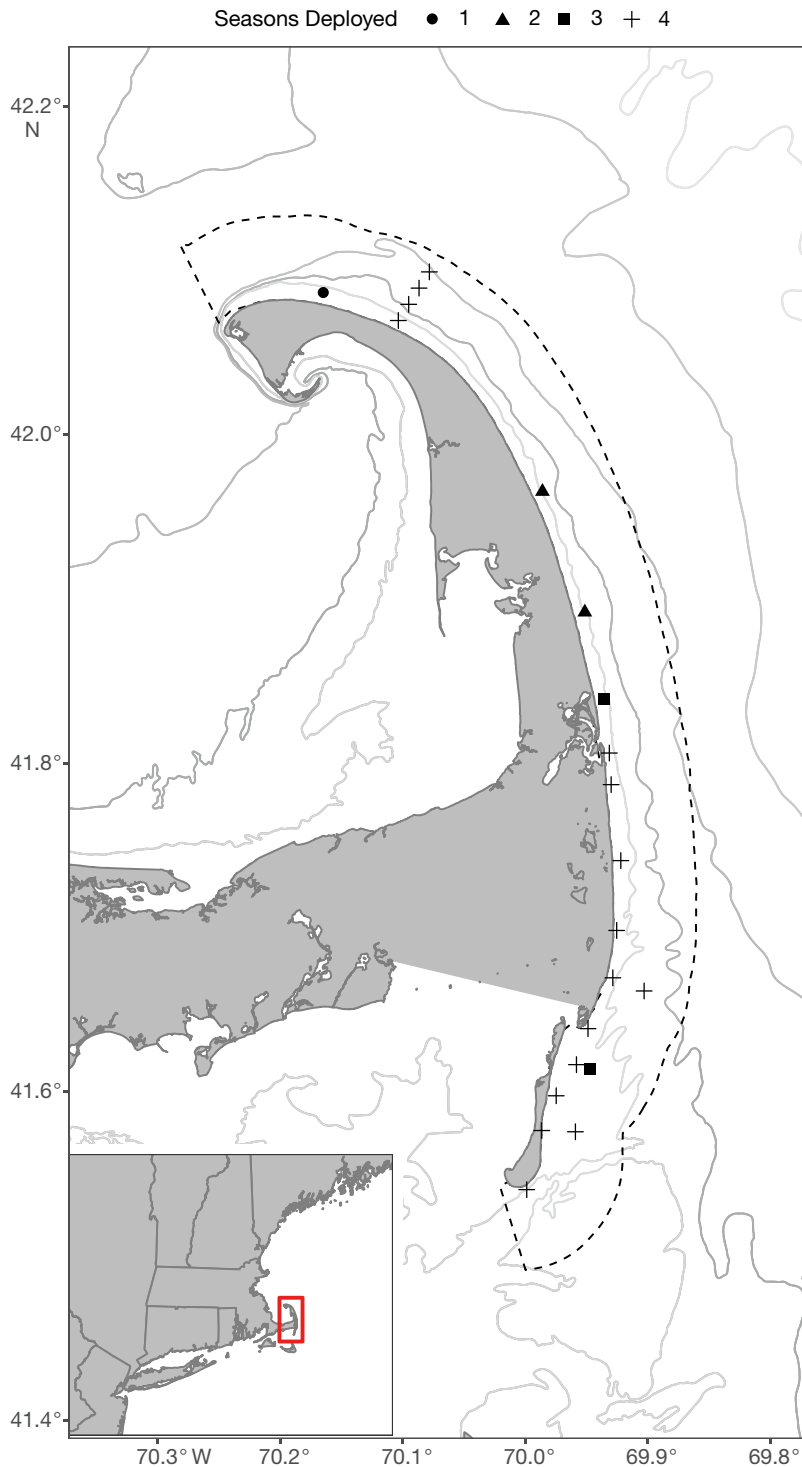


Fig. 1. Study area, showing the location of acoustic receivers deployed from 2015–2018 along the Atlantic-facing coast of Cape Cod, Massachusetts, USA. Grey lines radiating from the coastline: 15, 25, 40, and 90 m bathymetric contours; darker shades of grey: deeper depths; dashed line: survey area

camera (GoPro models Hero3 and Hero4) mounted on a fiberglass telescoping painter's pole was used to record underwater footage of free-swimming sharks.

A pilot study conducted during the summer and fall of 2014 proved this approach feasible (see Section 3); therefore, the survey was expanded and conducted seasonally from 2015–2018. Available tagging data indicated clear seasonal movement patterns and a high degree of variation in residency and habitat use (Skomal et al. 2017, Winton et al. 2021). Therefore, survey trips were conducted twice a week when conditions allowed from late June through October to capture the aggregation's seasonal dynamics and increase the chance that 'transient' individuals would be encountered.

A handheld GPS (Garmin GPSMAP 78sc) was used to record the boat's track for the duration of each trip as a measure of spatial variation in survey effort and the location of each shark encountered. Because we needed to assign the location of videoed encounters to the survey track for model fitting, we chose to use the research vessel's track as a measure of effort rather than that of the spotter plane. Although the plane's track may have provided a more appropriate measure of the survey's extent, the nature of our field operations required concise communication between the research vessel and the pilot, which rendered the coordinated collection of data across platforms practically infeasible.

At the time of each encounter, the total length (TL) of each shark was visually estimated to the nearest 0.3 m via expert consensus using the research vessel's pulpit length for scale (Skomal et al. 2017), unless water clarity and depth precluded estimation. When possible, sharks that were encountered during the survey were tagged with individually coded 69 kHz acoustic transmitters (Models V16-4x, V16-6x, or V16TP-6x; Innovasea Systems). Sharks were tagged externally while free-swimming (see Skomal et al. 2017 for details) to minimize tagging

effects and reduce the likelihood of altered movement behavior following capture (Bowlby et al. 2021), which could affect the probability of re-

encountering tagged individuals during subsequent survey efforts (Burgess et al. 2014). All tagging operations were conducted under Exempted Fishing Permits (SHK-EFP-11-04, SHK-EFP-12-08, SHK-EFP-13-01, SHK-EFP-14-03) issued by the National Marine Fisheries Service Highly Migratory Species Management Division and permits issued by the Massachusetts Division of Marine Fisheries.

## 2.2. Identification of individual white sharks

Video collection methods resulted in a large amount of footage that did not contain a shark. To expedite video processing, a custom algorithm was developed using an open-source, convolutional neural network that was trained to identify portions of the videos containing a shark and classify the body region captured (C. Rillahan, University of Massachusetts Dartmouth; <https://github.com/EminentCodfish/White-Shark-CNN-Classifer>). The resulting product converts a video to a set of labeled photographs. Sequences of photographs that contained distinguishing features were post-processed in Adobe Photoshop Lightroom Classic (Adobe Systems) to adjust white balance, color contrast, and exposure to improve image clarity.

Processed photographs were used to document and match each shark encountered with previously identified individuals. Full shots of both sides of the body were not always captured during each encounter, and a single feature could not be used for identification. Individuals were identified based on countershading and fin pigment patterns (Domeier & Nasby-Lucas 2007) as well as the dorsal fin profile, which is unique to each shark (Anderson et al. 2011). We modified the criteria developed by Domeier & Nasby-Lucas (2007) for white sharks at Guadalupe Island, Mexico, to define pigment pattern types for the gill flaps, the dorsal fin, the pelvic fin region, and the caudal fin. The sex of the shark, presence of tags, and scars or evidence of major injuries (e.g. propeller wounds, damaged fins, scoliosis) were used to confirm identifications. Unless claspers were visible, sex was only assigned if clear ventral footage of the pelvic fins was captured to definitively determine that the shark was female.

For each video, all features visible in the footage were classified, and the combination of scores were used to determine potential matches. Because pigment patterns are not identical on both sides of the body (Domeier & Nasby-Lucas 2007), each feature was scored on the right and left sides. In all, 9 fea-

tures were scored (see 'White Shark Catalog' at <https://shiny.atlanticwhiteshark.org/logbook/> for examples). Unique characteristics were then used to match the individual to previously identified sharks. If only partial footage of a shark was obtained and it could not be matched to a previously identified individual, it was cataloged as a 'potential' individual until additional footage was captured on subsequent trips. Only sharks with a minimum of 6 scored features were included in the final data set to ensure that individuals were not included as multiple sharks. Given the slow growth rate of the species (Natanson & Skomal 2015) and relatively short survey timeline, the TL of each identified shark was assigned as the mean of the TL estimates recorded during all encounters of that individual. Based on previously published estimates of size-at-maturity, 3 sex-specific maturity stages were assigned as defined by Bruce & Bradford (2012): 'juvenile' ( $\leq 3.0$  m); 'subadult' (males  $> 3.0$ – $3.6$  m; females  $> 3.0$ – $4.8$  m); and 'adult' (males  $> 3.6$  m; females  $> 4.8$  m). In cases where the sex of tagged individuals could not be determined, maturity stage was only assigned if the estimated TL was  $\leq 3.6$  or  $> 4.8$  m.

## 2.3. Seasonal monitoring for the presence of tagged sharks

Omnidirectional acoustic receivers (Models VR2W, VR2Tx, and VR2C; Innovasea Systems) were deployed along the Outer Cape from the late spring into the following winter in each year (Fig. 1). Though the exact dates of deployment and retrieval varied depending on weather conditions and logistics, deployments spanned the survey period in each season. Over the course of the study, the number of receivers increased with available funding (Fig. 1). Receivers were deployed at a depth of 1.3 m on surface buoys in water depths ranging from 4.5 to 12.0 m beyond the surf zone, where high ambient noise levels can dramatically reduce receiver detection ranges (Kessel et al. 2014); extensive range tests conducted in a portion of the array suggested that receivers had an average detection range of 400–500 m (B. Legare pers. comm.). Here, we considered only detection data collected during survey periods in each year. Acoustic detection data were downloaded following receiver retrieval, time-corrected, and scanned for false detections based on the criteria outlined by Pincock (2012) using the manufacturer's software (VUE v.2.4.0; <https://support.fishtracking.innovasea.com/s/downloads>).

## 2.4. Model description

Our goal was to investigate the seasonal dynamics and estimate the overall size of Cape Cod's white shark population while accounting for movement-related sources of bias characteristic of white shark aggregations. To do so, we extended the open SCR model developed by Glennie et al. (2019) to account for temporary emigration and to integrate acoustic telemetry data, as described below. As with conventional capture–recapture models, SCR models are formulated in terms of individual encounter histories that specify whether an individual was encountered on each survey or not but also extend them to account for variation in space use. We begin by describing the SCR approach for a single survey period and build upon that model to describe how movements into and out of the area are accounted for between survey periods using an open formulation.

Conceptually, SCR approaches consider observed encounters as the realization of a latent spatial point process that is biased by the observation process (here, the location and duration of survey efforts; Royle et al. 2014). The underlying point process is assumed to describe the distribution of individual activity centers during the sampling period, which cannot be directly observed but must be inferred from the observed encounters and so are modeled as latent variables (i.e. random effects). The location of the activity center of individual  $i$  during each sampling period  $t$ ,  $\mathbf{s}_{it}$ , is typically modeled as the realization of a homogeneous Poisson point process:

$$\mathbf{s}_{it} \sim \text{Uniform}(\mathbf{S}) \quad (1)$$

where  $\mathbf{S}$  is the sampled area (often referred to as the 'state-space' in SCR models; Royle et al. 2014). The estimated distribution of activity centers can then be used to estimate the population size in  $\mathbf{S}$  in each period,  $N_t$ , as:

$$N_t \sim \text{Poisson}(\mu_t \|\mathbf{S}\|) \quad (2)$$

where  $\mu_t$  is the density of the point process and  $\|\mathbf{S}\|$  is the area of  $\mathbf{S}$ . The resulting point pattern is informed by the observed encounters and can differ markedly from uniformity when individuals aggregate in relation to unmeasured factors (Royle et al. 2014), such as the dynamic distribution of seal haulout sites (Moxley et al. 2017).

Given our irregular search pattern, we used a model developed to infer density from encounter histories collected using similarly opportunistic searches

by detector dogs (Russell et al. 2012, Thompson et al. 2012). The approach involves gridding  $\mathbf{S}$  and using the location of grid cells visited in each survey as conceptual 'traps' that can shift between sampling periods, which are often termed primary occasions (Pollock 1982). For each survey, individual encounter histories were specified as 1 if individual  $i$  was encountered in grid cell ('trap')  $j$  and 0 if it was not encountered. We summed the number of surveys that each individual was encountered in each grid cell,  $y_{ijt}$ , over the sampling period  $t$  and modeled it as the outcome of a binomial random variable:

$$y_{ijt} \sim \text{Binomial}(K_{jt}, p_{ijt}) \quad (3)$$

where  $K_{jt}$  is the number of individual survey trips in which grid cell  $j$  was visited during  $t$ , and  $p_{ijt}$  is the occasion-specific probability of encountering each individual in each grid cell visited.

The premise of the SCR approach is that any individual with an activity center in  $\mathbf{S}$  during survey period  $t$  may have been encountered, but was more likely to have been encountered if survey efforts overlapped the core area used by the individual during  $t$ . For our unstructured survey, we expected higher encounter rates for individuals with core use areas close to grid cells with high sampling intensities (Thompson et al. 2012). To accommodate variation in survey effort, we modeled  $p_{ijt}$  using the complementary log–log ('cloglog') link function, which relates the number of expected encounters under a Poisson model  $\lambda_{ijt}$  to the probability of encountering an individual at least once as:

$$\Pr(y_{ijt} > 0) = p_{ijt} = 1 - \exp(-\lambda_{ijt}) \quad (4)$$

which implies that:

$$\text{cloglog}(p_{ijt}) = \log[-\log(1 - p_{ijt})] = \log(\lambda_{ijt}) \quad (5)$$

and allows for effort to be included as an offset term. Using functions available in the 'sf' (Pebesma 2018) and 'analyzeGPS' (Plesnik 2015) packages in R version 4.0.1 (R Core Team 2020), we assigned vessel tracks and individual encounters to grid cells in each sampling occasion. We calculated the length of the vessel's survey path through each grid cell in each sampling period as a measure of effort (Thompson et al. 2012). When environmental conditions were not ideal, survey track lengths were shorter because movements were restricted (e.g. by sea state) or because sharks were not being spotted (e.g. when water turbidity was high); therefore, we considered survey effort as

a cumulative proxy for environmental conditions impacting encounter rates (i.e. sea state, cloud cover, water clarity) rather than including individual terms for additional covariates that would be confounded with effort. Prior to model fitting, all georeferenced data sets and the gridded state space were projected into the Massachusetts State Plane Coordinate System (EPSG 26986, which has units of meters) and scaled by 10 km to reduce run times.

In addition to accounting for variation in effort, we were interested in determining if encounter rates changed over the course of the survey. We modeled variation in the expected number of encounters as:

$$\log(\lambda_{ijt}) = \beta_{0,\text{year}} - \frac{1}{2\sigma^2} \|\mathbf{x}_j - \mathbf{s}_{it}\|^2 + \beta_1 \log(\text{effort}_{jt}) \quad (6)$$

where  $\beta_0$  is the year-specific baseline encounter rate, or the number of encounters that would be expected at the individual's activity center (i.e. at a distance of zero);  $\sigma$  is the standard deviation of a bivariate normal distribution that describes the decrease in encounter probability with the Euclidean distance between the grid cell center  $\mathbf{x}_j$  and the individual's center of activity  $\mathbf{s}_{it}$  during occasion  $t$ ; and  $\beta_1$  represents the multiplicative effect of survey effort on encounter rates (Thompson et al. 2012). Because not all grid cell traps were visited in every survey month, we added 1 km to survey track lengths in each grid cell to avoid convergence issues associated with taking the log of zero; we also centered effort so that the base encounter rate corresponded to mean survey effort. As specified, the model allowed activity centers to move independently between primary periods to reflect the high mobility of the species in the region (Gowan et al. 2021).

#### 2.4.1. Open population model

Open SCR models link a time series of closed SCR models to account for demographic processes that influence surveyed populations over time and space, and assume that encounter probabilities depend not only on space use but also on the state that an individual is in at a given point in time (Glennie et al. 2019). We formulated an open SCR model using a robust design approach (Pollock 1982) to ensure enough data for estimating variation in encounter rates and population size over time. Individual surveys were grouped by survey month into 19 'primary' occasions, which included between 3 and 13 individual surveys (often termed 'secondary' occasions). In each primary occasion, we assumed that

white sharks were in one of 3 states ('before', 'present', and 'away') that would impact their encounter probability as described below. Individuals could transition among states between primary periods but were assumed to remain in a given state within them (Pollock 1982).

Prior to visiting the Cape Cod aggregation site, white sharks would not be available to sampling efforts and were considered to belong to the 'before' state. Fisheries catch data do not suggest white sharks pup in the nearshore waters off Cape Cod (Curtis et al. 2014); therefore, we assumed that all sharks that were not yet part of the surveyed population were recruited from outside the area, with primary occasion-specific probability  $\gamma_t$ . We note that  $\gamma_t$  represents the probability that an individual enters the surveyed population at primary occasion  $t$  given that it had not entered the population prior to that occasion, not the overall probability of entry in each period,  $\alpha_t$ , which was derived following Glennie et al. (2019). Once they entered the surveyed population, white sharks were considered 'present' and would be encountered (or not) depending on their space use and the location of survey efforts as described above. An individual that was present during a primary occasion remained in the surveyed area with probability  $\phi_t$  or emigrated (entering the 'away' state) with probability  $1 - \phi_t$ . Individuals that were previously part of the surveyed population but 'away' either returned to the area between primary occasions with probability  $\eta_t$  or remained away with probability  $1 - \eta_t$ ; we note that permanent emigration of an individual is confounded with mortality (Pollock 1982). Following Glennie et al. (2019), we assumed the state of an individual depended only on its state during the previous primary period and formulated the 'open' component as a non-homogeneous hidden Markov model (Zucchini & MacDonald 2009) with time-varying transition probability matrix:

$$\Gamma_t = \begin{bmatrix} 1 - \gamma_t & \gamma_t & 0 \\ 0 & \phi_t & 1 - \phi_t \\ 0 & \eta_t & 1 - \eta_t \end{bmatrix} \quad (7)$$

where the first, second, and third rows and columns correspond to the states 'before', 'present', and 'away', respectively. An individual's state in primary occasion  $t$  was modeled as the outcome of a Bernoulli random variable that depended on their state in occasion  $t - 1$ . Because individuals could only be in the 'before' or 'present' states in the first primary occasion, the initial distribution of the Markov chain depended only on the probability of entry and corre-

sponded to the first row of  $\Gamma_t$ . Given the progression of states, individuals could first move into the 'away' state during the second primary occasion and could not return until the third occasion; therefore,  $\eta_t$  was specified as 0 for  $\Gamma_1$ .

Our survey was designed to target months when white sharks seasonally aggregate in the nearshore waters along Cape Cod, so we did not sample during every month of the year. Consequently, our use of a monthly time step for primary occasions resulted in irregular time steps between the last primary occasion in one year and the first occasion in the next. Continuous time versions of hidden Markov models exist but assume that transition probabilities remain constant over the time steps spanned by the gaps (Glennie et al. preprint <https://doi.org/10.48550/arXiv.2106.09579>). For our application, this would imply that  $\gamma_t$ ,  $\phi_t$ , and  $\eta_t$  were constant from the end of October through the beginning of June, which is unreasonable given the species' seasonal use of the site (Skomal et al. 2017, Winton et al. 2021). Therefore, we chose to use the discrete time parameterization described above, but note that the interpretation of transition probabilities between seasons is different from those within a given season. Between seasons,  $\gamma_t$  represents the probability of a new individual entering the surveyed population from the late fall into the early spring,  $\phi_t$  is the probability that an individual that was present in October and presumably migrated for the winter was back again the subsequent June, and  $\eta_t$  is the probability an individual that was not present in October had returned in June.

The probability of encountering an individual in each primary occasion depended on its state. Individuals in the 'before' and 'away' states were not available to survey efforts and therefore had an encounter probability of zero. Any individual that was 'present' was detected with marginal probability  $\bar{p}_t$  which was computed following Dupont et al. (2021). First, we calculated the probability that an individual with an activity center  $s_i$  was encountered in any of the sampled grid cell 'traps'  $X$  during primary occasion  $t$  as:

$$\bar{p}_t(s_i, X) = 1 - \prod_{j=1}^J [1 - p_t(s_i, X)] \quad (8)$$

Then, we computed the marginal probability of encounter as the area-weighted average over all grid cells  $G$ :

$$\bar{p}_t(X) = \sum_{g=1}^G \bar{p}_t(s_i, X) \frac{\text{Area}(g)}{\text{Area}(S)} \quad (9)$$

The resulting time-varying, state-dependent encounter probability matrix was:

$$P_t = \begin{bmatrix} 0 & 1 \\ \bar{p}_t & 1 - \bar{p}_t \\ 0 & 1 \end{bmatrix} \quad (10)$$

where the first column corresponds to the probability of encounter and the second to the probability of not being encountered, and the 3 rows correspond to the same states as specified for  $\Gamma_t$  in Eq. (7) above.

#### 2.4.2. Integrating acoustic telemetry data

While the states of most individuals could only be partially observed (i.e. during occasions when they were encountered) and therefore were inferred based on observed encounter histories, the states of tagged individuals could be assigned with reasonable certainty. To incorporate 'known' states for tagged individuals, we integrated data collected during a concurrent acoustic telemetry study into the open component of the model. Acoustic detection data for each tagged individual were binned by survey month and used to determine if individuals were present in the study area in each primary occasion. Because tagged sharks cannot be detected prior to transmitter deployment or after battery expiration or transmitter loss, we used tag deployment dates and individual detection histories to determine the time period during which a tagged shark was 'available' to be detected by a receiver. Tag shedding rates are currently unknown for our program but are likely non-negligible (Chapple et al. 2016); therefore, we conservatively defined the effective monitoring period for each shark tagged as the time between tagging and the last valid detection in any receiver array along the eastern coast of the USA or Canada until 31 October 2018, the end of the survey period (G. B. Skomal & M. V. Winton unpubl. data). Sharks that were detected anywhere in our array during primary occasion  $t$  were considered 'present' and those that were only detected outside of the array were considered 'away' and unavailable to survey efforts. Given the nature of acoustic telemetry data, tagged sharks were not necessarily detected each month; individuals that were not detected were not assigned a state. In other words, the state of tagged sharks was considered known if an individual was detected during that primary occasion and unknown if it was not detected.

We emphasize that we used acoustic detection data only to determine if an individual visited the surveyed area at some point in each primary occasion and not to determine the length of residency or



whether a tagged shark remained within the surveyed area throughout the entire period. Given the movement capabilities of the species, many individual white sharks would move in and out of the surveyed area over the course of a given month (Skomal et al. 2017). However, the central premise of SCR models—that individual encounter probabilities depend on an animal’s center of activity during each primary period—provides an intuitive solution for accounting for such transient individuals. Conceptually, transient individuals are considered as individuals that primarily used regions beyond the surveyed area during occasion  $t$  and were, therefore, infrequently encountered (Royle et al. 2016).

#### 2.4.3. Parameter estimation and simulation testing

We used maximum likelihood methods to estimate parameters using custom functions implemented in the software Template Model Builder (TMB; Kristensen et al. 2016), a recently developed R package (R Core Team 2020) that uses the Laplace approximation and automatic differentiation to efficiently fit complex hierarchical models to large data sets. As it is easily customizable and much less computationally demanding than the Bayesian approaches that have been used to fit most open SCR models developed to date (see Royle et al. 2014 for a review, Gowan et al. 2021), TMB makes it feasible to fit and conduct model selection for applications with many primary occasions, such as that described here. Code for fitting the model described in TMB can be found on the Atlantic White Shark Conservancy’s publicly available GitHub page (<https://github.com/AtlanticWhiteSharkConservancy>).

As formulated, the likelihood consists of 2 components relating to the ‘open’ and ‘closed’ portions of the model that are estimated jointly. For the hidden Markov model describing transition probabilities between states, we used the forward algorithm to evaluate the likelihood (Zucchini & MacDonald 2009). To incorporate known states for tagged individuals, we constrained encounter probabilities when the state of the individual was considered known to limit transitions between survey periods to the known states. For the SCR model describing variation in encounter probabilities within each primary period, we implemented the Poisson-integrated version of the likelihood (Borchers & Efford 2008) to estimate the marginal likelihood and abundance in each primary occasion. As for the calculation of the marginal encounter probability, conditional likelihoods for each

grid cell were weighted by area to account for differences in the size of grid cells bordered by the habitat mask or the boundary of the state-space  $\mathbf{S}$ , which typically extends beyond the surveyed area in order to encompass the activity centers of all individuals potentially exposed to sampling (Royle et al. 2014).

In the case of white sharks, we expected  $\mathbf{S}$  would need to be quite large given the movement capacity of the species (Skomal et al. 2017). We conducted a series of exploratory fits using the closed portion of the model (i.e. the model estimating population size in each primary occasion) to determine the appropriate buffer and grid cell area (Royle et al. 2014, Glennie et al. 2019). Starting with a 5 km buffer and a 100 km<sup>2</sup> grid cell size, we iteratively expanded the survey area at 5 km increments (masking out portions of grid cells to prevent activity centers from occurring on land) until density estimates for each primary occasion stabilized. We also plotted the effective sampled area of subsequent buffer sizes to determine the buffer width that would encompass the activity centers of all individuals potentially exposed to sampling (Royle et al. 2014); this was achieved with a buffer width of 25 km<sup>2</sup>, which corresponded to an area of 6811 km<sup>2</sup> for  $\mathbf{S}$  (Fig. S1 in the Supplement at [www.int-res.com/articles/suppl/m715p001\\_supp.pdf](http://www.int-res.com/articles/suppl/m715p001_supp.pdf)). We then did the same for grid cells, decreasing the grid cell area in 25 km<sup>2</sup> increments to evaluate the relative influence of grid resolution on density estimates. Parameter estimates were relatively constant at grid cell sizes from 100 down to 25 km<sup>2</sup>; therefore, we used a grid cell size of 100 km<sup>2</sup> for model fitting to reduce computation time.

To determine the impact of accounting for variation in space use, movements into and out of the survey region, and integrating acoustic telemetry data on demographic parameter estimates, we conducted simulation testing. We used the distribution of actual survey effort in each monthly primary occasion and parameter estimates from preliminary model fits to generate encounter histories for a superpopulation ( $N_{\text{super}}$ ) of 1000 individuals assuming constant  $\beta_0 = -3.0$ ,  $\sigma = 1.5$ ,  $\beta_1 = 0.5$ ,  $\phi_t = 0.6$ , and  $\eta_t = 0.2$  for ease of interpretation. We used a multinomial distribution to generate the number of individuals entering the surveyed population prior to each occasion, with  $\alpha_0 = 0.200$  and all other  $\alpha_t = 0.047$ . For simulations, we assumed that untagged individuals encountered during each sampling occasion were tagged with probability = 0.12; this value was based on the mean ratio of sharks tagged to those that were not tagged in each survey trip.

To evaluate the impact of integrating acoustic telemetry data, we made several simplifying assumptions regarding tagged individuals. We assumed that tagged individuals did not shed their tags and that their state could be definitively determined in each subsequent time step. We also assumed that tagged individuals were representative of the broader population. While these assumptions represent an idealized scenario that is unlikely achievable in practice, they were necessary to disentangle the impact of the additional information available provided by tagged individuals from factors that complicate the interpretation of any acoustic telemetry study.

We fit 5 versions of the model to assess their performance and the implications of assumptions often applied in white shark capture–recapture studies: (1) the telemetry-integrated open SCR model allowing for temporary emigration as described above; (2) a standard (i.e. non-telemetry-integrated) version of the same model; (3) a standard open SCR model that did not allow for temporary emigration (similar to the model formulated by Glennie et al. 2019); (4) a non-spatial version of the model allowing for temporary emigration that did not account for individual variation in space use or survey effort; and (5) a closed SCR model that estimated  $N_t$  independently and did not account for movements between primary periods. To assess performance, we fit all 5 models to 100 simulated data sets and calculated the difference between the estimated and true value for each estimated model parameter as well as the derived  $N_{\text{super}}$  size.

### 2.5. Estimating white shark abundance and seasonal dynamics

Our integration of telemetry data implies that tagged and untagged animals transitioned between states at the same rates. This assumption may not be appropriate for white sharks, which exhibit varying degrees of residency at seasonal aggregation sites (Jewell et al. 2013, Winton et al. 2021). ‘Resident’ sharks that regularly use and return to a site would be more available to tagging efforts than transient individuals that are only brief visitors (Hewitt et al. 2018), which could bias estimates of movement probabilities as well as the resulting estimates of abundance. To determine if the movements of tagged individuals were consistent with those of the broader population, we used the Akaike information criterion (AIC; Akaike 1973) to compare the fit of the model described above with and without a tagging effect on

$\phi_t$  and  $\eta_t$ . To do so, we included an additional parameter for each term representing variation among tagged and untagged individuals:

$$\text{logit}(\phi_{t,\text{tag}}) = \mu_t + \mu_1 \text{tag} \quad (11)$$

and

$$\text{logit}(\eta_{t,\text{tag}}) = \rho_t + \rho_1 \text{tag} \quad (12)$$

where  $\text{tag} = 0$  for individuals that were not tagged during the course of the study and 1 for those that were.

We also aimed to characterize the temporal dynamics of the aggregation and used AIC values to compare the fit of models with various types of time-specific parameters. In particular, we were interested in determining (1) if there was evidence of a change in baseline encounter rates over the course of the survey, which could suggest changes in activity patterns of white sharks at the aggregation site over time or changes in survey efficiency, and (2) if immigration and emigration rates were constant over time, varied between each primary occasion, or varied predictably over the course of the season, reflecting ‘pulses’ of immigration and emigration into and out of the area. For (1), we compared the fit of models that included and did not include the year-specific baseline encounter rate in Eq. (6). For (2), we compared models with the encounter model selected in (1) with primary occasion-specific, month-specific, or constant  $\phi$  and  $\eta$ . We inspected the final gradient value for parameters and confirmed the models had converged prior to model selection.

Based on the selected model, the total number of white sharks using the Cape Cod aggregation site over the survey period ( $N_{\text{super}}$ ) was derived by dividing the estimated abundance in the first primary occasion,  $N_1$ , by the probability of entering the surveyed population prior to that occasion,  $\alpha_0$  (Schwarz & Arnason 1996). The full list of estimated and derived parameters can be found in Table 1.

### 2.6. Model evaluation

As residual diagnostics associated with open SCR models can be difficult to interpret, we used a parametric bootstrapping approach to assess the fit of the selected model (Russell et al. 2012). We used the selected model to generate 100 data sets and refit the model to simulated values. To evaluate whether the assumption of uniformly distributed activity centers was sufficient, we computed the Freeman-Tukey

Table 1. Estimated and derived parameters for the open spatial capture–recapture model described in the text

Parameter	Symbol	Indexed by
<b>Spatial capture–recapture model</b>		
Baseline encounter rate	$\beta_0$	Survey year
Survey effort	$\beta_1$	Constant
Standard deviation of bivariate normal detection function	$\sigma$	Constant
Individual activity center (random effect)	$s_{it}$	Individual, primary occasion
Abundance	$N_t$	Primary occasion
<b>Open population model</b>		
Probability of entering surveyed population given not yet entered	$\gamma_t$	Primary occasion
Probability of remaining in surveyed area	$\phi_t$	Primary occasion
Probability of returning to surveyed area	$\eta_t$	Primary occasion
<b>Derived</b>		
Probability of entering surveyed population	$\alpha_t$	Primary occasion
Superpopulation size	$N_{\text{super}}$	Constant

(FT) fit statistic for the estimated number of activity centers occurring in each grid cell  $g$  in each primary occasion as:

$$FT_{1,t}(C_{gt}) = \sum_g^G [\sqrt{C_{gt}} - \sqrt{E(C_{gt})}]^2 \quad (13)$$

where  $E(C_{gt})$  is the mean count of activity centers in each grid cell (Royle et al. 2014). To assess the fit of the observation model, we calculated the same statistic using the observed and expected number of encounters for each individual in each grid cell ‘trap’:

$$FT_{2,t}(Y_{ijt}) = \sum_j^J [\sqrt{Y_{ijt}} - \sqrt{E(Y_{ijt})}]^2 \quad (14)$$

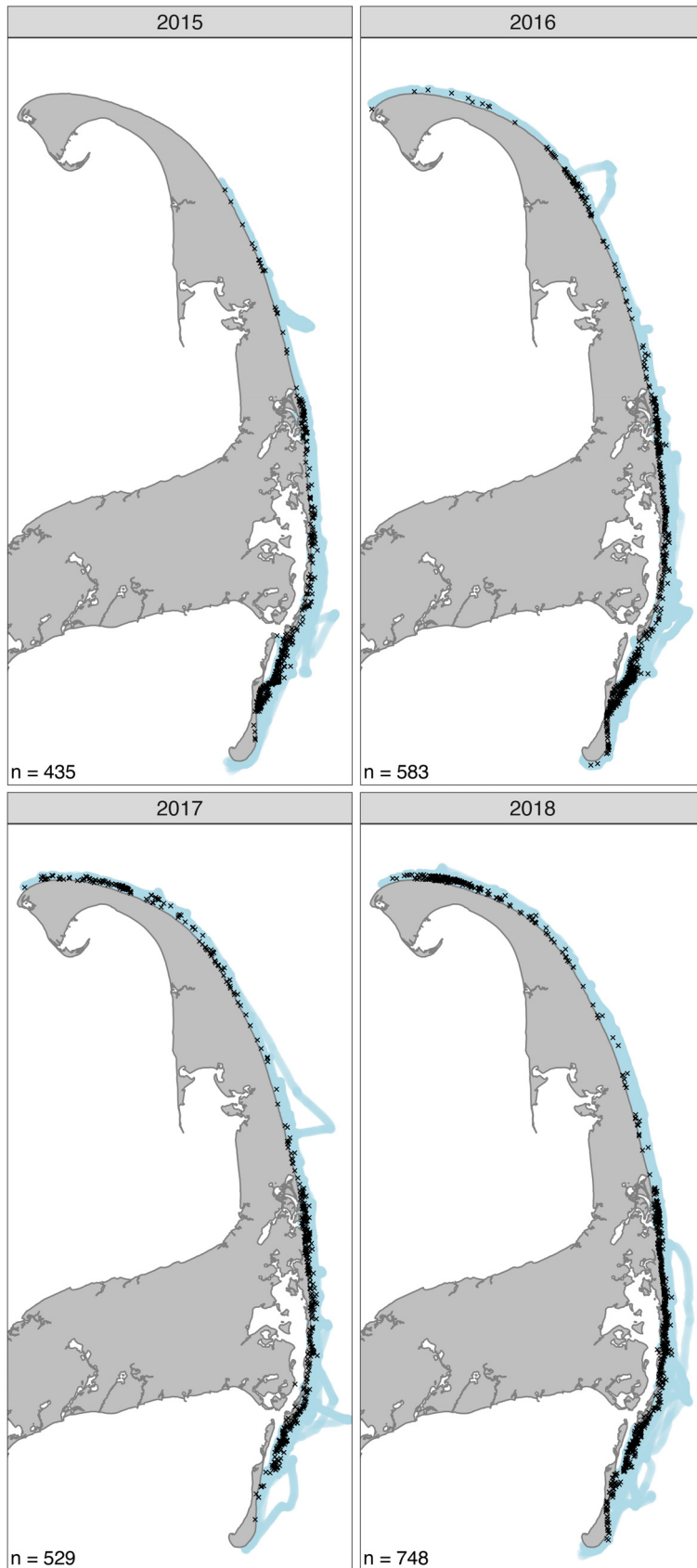
Both fit statistics were calculated for the selected model fit to the observed data set, and compared to the distribution of the value for data sets simulated under the correct model to determine if the statistical model applied in the analysis could generate the observed data (Royle et al. 2014).

### 3. RESULTS

During the 137 survey trips conducted during the summer and fall of 2015–2018, we encountered white sharks 2295 times and collected a total of 2803 videos. Sharks were encountered along the entirety of Cape Cod’s Atlantic-facing coastline (Fig. 2) in water temperatures ranging from 8.7 to 20.9°C (mean  $\pm$  SD: 15.6  $\pm$  2.1°C) and at depths ranging from 1.2 to 12.2 m (mean  $\pm$  SD: 3.9  $\pm$  1.4 m). In total, 361 of the videos collected (13%) did not contain footage of a shark; this typically occurred when sharks were in water deeper than the length of the camera pole

(~4.5 m). Of the 2442 videos that contained footage of a shark, 130 (5%) were not of sufficient quality for identifying features to be classified. Similar to Domeier & Nasby-Lucas (2007), we found that pigment patterns were stable across years, though slight changes in gill and caudal pigment patterns did occur in a few individuals. During some periods, patches of algal growth on the pelvic fins or gills obscured markings; however, given our use of multiple features, this did not affect our ability to identify individuals.

We identified a total of 408 individual white sharks from underwater video footage collected from 2014–2018. Of those individuals, 393 were encountered over the course of the survey and included in the model used to estimate abundance. The other 15 individuals were identified during the 2014 pilot study and were not resighted in subsequent survey years. An additional 103 ‘potential’ individuals were cataloged but did not have the minimum number of features documented to definitively determine that they were not included as multiple sharks. Sharks that were only encountered during the pilot study or identified as potential individuals were omitted from the data set used to estimate abundance and are not included in the summaries that follow. Identified sharks had estimated TLs ranging from 1.8 to 4.9 m (Fig. 3), with more males encountered ( $n = 189$ ) than females ( $n = 143$ ), though the difference is likely in part due to the visibility of claspers in larger males. Based on sex-specific estimates of size-at-maturity, the majority of the individuals identified were immature ( $n = 315$ ; 119 juveniles and 196 subadults), with a larger number of mature males ( $n = 52$ ) encountered than females ( $n = 2$ ). We were unable to deter-



mine the sex of 61 individuals, and, consequently, the maturity stage of 16 individuals with estimated TLs between 3.6 and 4.8 m. TL was not estimated for 6 individuals due to the depth of the shark or poor visibility.

Of the 393 individuals encountered during the survey, 53 were first encountered during the pilot study in 2014, 62 in 2015, 72 in 2016, 92 in 2017, and 114 in 2018. In total, 106 individuals were documented in 2015, 135 in 2016, 177 in 2017, and 242 in 2018. Roughly two-thirds ( $n = 261$  individuals) were encountered on more than one survey trip (Fig. 4a) and almost half ( $n = 167$ , 43%) were encountered in multiple survey years (Fig. 4b). While the majority of individuals were encountered fewer than 5 times ( $n = 328$ ) and in only one year of the survey ( $n = 226$ ), some individuals were sighted on more than 10 survey trips ( $n = 25$ ). Of those 25, all but one individual were encountered in 3 or more years. The observed encounter histories suggest a mix of transient individuals that are only brief visitors and more resident sharks that regularly use the nearshore waters along Cape Cod.

We tagged 79 white sharks with acoustic transmitters over the course of the survey and encountered 8 individuals that had been tagged in previous years. Of those 87 individuals, 84 (97%) were detected in the waters along Cape Cod in at least one survey month. Individual detection histories spanned 1–19 survey months (Table S1), with an accumulated total of 709 monitored months across all tagged sharks. Tagged individuals were detected in our array and considered 'present' in 60% of monitored months ( $n = 425$ ) but were only encoun-

Fig. 2. Location of white shark encounters during all 4 years of the photographic identification survey. Cross marks: white shark locations; blue lines: research vessel tracks, which were used as a measure of survey effort. The number of encounters in each survey season (which does not equate to the number of individuals encountered) is indicated in the bottom left-hand corner of each panel

tered during survey trips in roughly half of those months ( $n = 212$ , 50%). No individuals assigned to the 'away' state were encountered on survey trips, but 5 individuals were encountered during months in which they were not detected in any array and were not assigned a status, which suggests not all tagged sharks that were present in the area were detected by our receiver array. While the number of tagged individuals 'available' to be detected increased over the course of the survey ( $n = 26$  in 2015, 38 in 2016, 57 in 2017, and 67 in 2018), the proportion of available individuals detected in our array remained high among years (92% in 2015, 82% in 2016, 77% in 2017, and 87% in 2018). Tagged individuals were present in all survey months and exhibited a high degree of variation in their occurrence in our array, both within and among years (Table S1). On average, individual tagged sharks were detected in our array and considered 'present' for 2.7 mo (range: 0–5 mo), 'away' for 1.4 mo (range: 0–4 mo), and could not be assigned a state for 2.4 mo (range: 0–5 mo) within a given survey season. Of the sharks that were tracked in at least 2 survey seasons ( $n = 56$ ), all but 11 (19%) were detected in multiple years.

### 3.1. Simulation testing

Our study-specific simulations indicated that the telemetry-integrated open SCR model generated the most reliable abundance estimates (Model 1 in Fig. 5h). As expected, integrating known states for tagged individuals improved estimates related to movements into and out of the surveyed area (Fig. 5f,g), which, in turn, reduced bias in parameter estimates related to the encounter process (Fig. 5a,b,c) due to the link between the closed and open components of the model. However, it did not completely negate bias in all parameter estimates, likely reflecting the complexity of our unstructured sampling scheme and the large number of primary occasions. In particular, the model underestimated the probability that an individual entered the surveyed population prior to the first primary occasion (Fig. 5d), which consequently inflated the resulting estimate of the number of individuals visiting the aggregation site over the duration of the survey (Fig. 5i). It seems plausible that increasing the proportion of individuals tagged would further reduce bias; however, this would not have been reflective of our sampling process and so was not investigated further here.

Even in the absence of telemetry data, all model parameters were identifiable and were reasonably

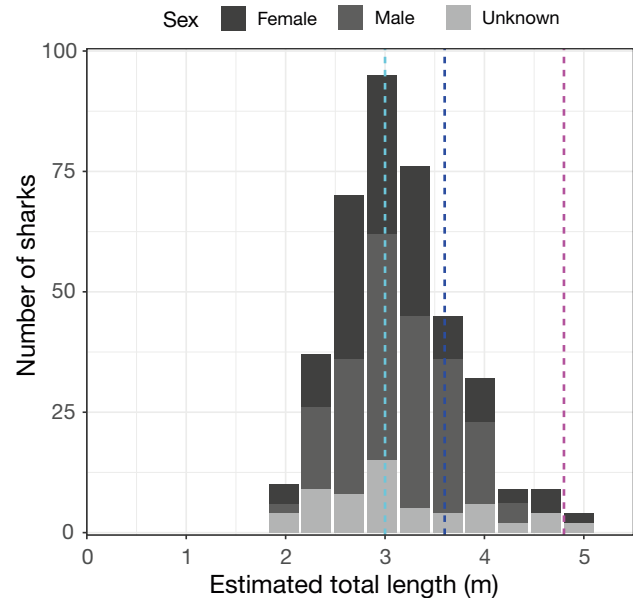


Fig. 3. Total length frequency distribution of 387 individual white sharks identified from footage collected off the coast of Cape Cod, Massachusetts, between 2015 and 2018. The length of 6 additional individuals could not be estimated. Cyan dashed line: total length at which individuals transition from juveniles to sub-adults; blue dashed line: median size-at-maturity for males; magenta dashed line: median size-at-maturity for females (Bruce & Bradford 2012)

well recovered by the open SCR model used to generate simulated data sets, though estimates exhibited some degree of bias (Model 2 in Fig. 5). Estimates of  $\phi_t$  and  $\eta_t$  were generally lower than the true value (Fig. 5f,g), implying this model estimated fewer individuals that entered the surveyed population would remain in or return to the area between primary occasions. In other words, the open SCR model that did not incorporate known states for tagged individuals assumed that fewer individuals that were 'present' remained or that were 'away' returned to the surveyed area than did in the simulated scenario. Consequently, fewer individuals were assumed to be 'present' and available for sampling in each primary occasion, inflating individual encounter rates (Fig. 5a,b) and underestimating the impact of survey effort (Fig. 5c). While overall bias was non-negligible, it was low and did not dramatically impact estimates of  $N_t$  or  $N_{\text{super}}$  in comparison to the telemetry-integrated model (Fig. 5h,i).

When temporary emigration and spatial variation in individual habitat use and survey effort were not accounted for, estimates of most parameters were biased. Under the model without temporary emigration (Model 3 in Fig. 5), individuals were assumed to remain within the state space until they permanently left the surveyed population, resulting in substantial

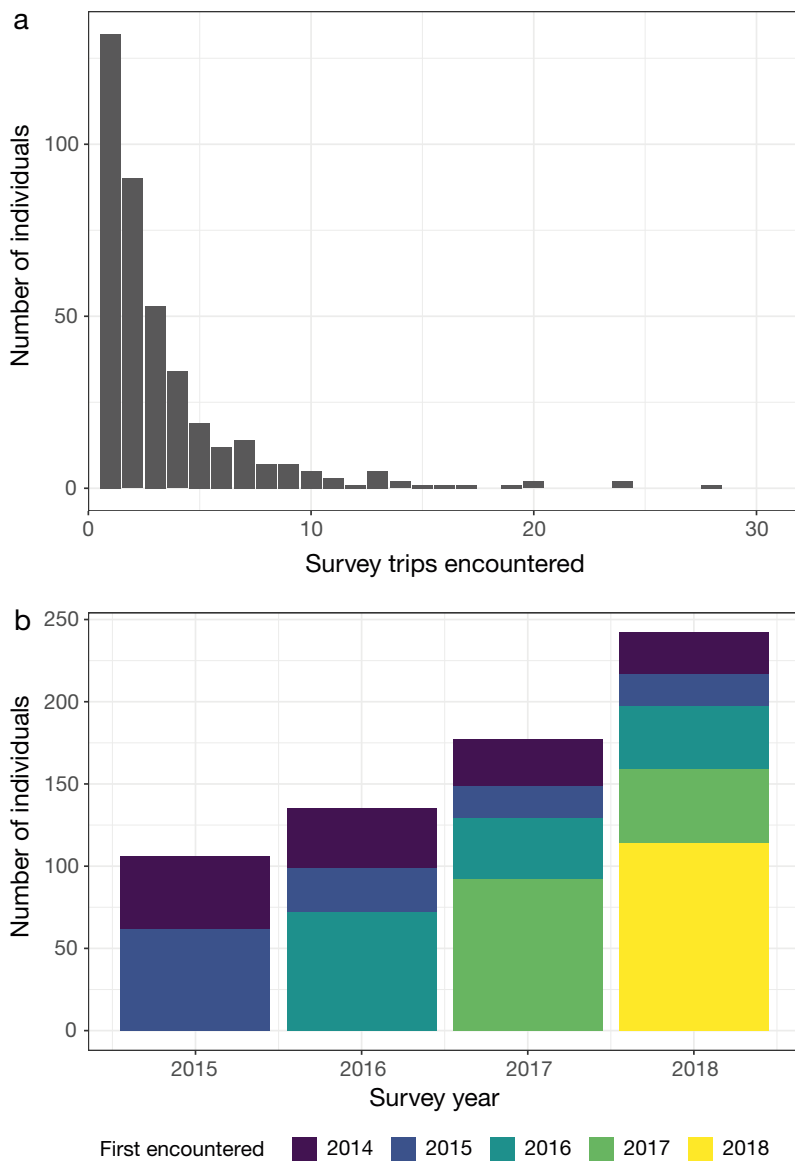


Fig. 4. (a) Total and (b) yearly encounter frequency of 393 individual white sharks identified from footage collected off the coast of Cape Cod, Massachusetts, during 137 survey trips conducted between 2015 and 2018

overestimation of  $\phi_t$ . Because the model assumed that individuals that did, in fact, temporarily migrate out of the area remained but were not encountered, more individuals were estimated to be 'present' and available for sampling in each primary occasion than in the true simulated scenario, resulting in deflated individual encounter rates (Fig. 5a) and, consequently, overestimates of abundance (Fig. 5h,i). In contrast, the model ignoring spatial variation in individual habitat use and survey effort (Model 4 in Fig. 5) underestimated abundance (Fig. 5h) as well as the probability that 'present' individuals would remain (Fig. 5f) or 'away' individuals would return (Fig. 5g).

Because Model 4 assumed that all individuals were equally likely to be encountered in all grid cell 'traps', the model could not account for individuals that primarily used habitat beyond the surveyed area despite producing an unbiased estimate of  $\beta_0$  (Fig. 5a). However, the resulting estimate of  $N_{\text{super}}$  was only slightly more biased than the models that accounted for spatial variation in encounter rates. The closed SCR model (Model 5 in Fig. 5) produced nearly unbiased estimates of all parameters related to the encounter process (Fig. 5a,b,c) but could not account for movements between primary periods and so could not be used to estimate  $N_{\text{super}}$  (Fig. 5i).

### 3.2. Estimates of abundance and seasonal dynamics

Comparison of the telemetry-integrated open SCR models that did and did not include a term for tagged individuals indicated evidence of difference in state transition probabilities ( $\phi_t$  and  $\eta_t$ ) between tagged and untagged sharks (Table 2), with tagged sharks more likely to remain in ( $\mu_1 = 2.42$ ; 95% CI = 1.85–3.04) and return to ( $\rho_1 = 0.27$ ; 95% CI = -0.13–0.66) the surveyed area between primary occasions, though we note the confidence limits for  $\rho_1$  included 0, indicating limited evidence of difference. This suggests that movements of tagged individuals into and out of the surveyed area were not representative of the

broader population; therefore, we used the standard (i.e. non-telemetry-integrated) version of the open SCR model for model selection and inference.

During AIC-based selection for the encounter component of the model, we found that dropping the year-specific baseline encounter rate improved relative fit (Table 2). In contrast, simplifying the temporal structure of the open component of the model reduced relative fit (Table 2). The selected model suggested no evidence of change in baseline individual encounter rates over the years the survey was conducted and that movements into and out of the region did not vary predictably over the course of the

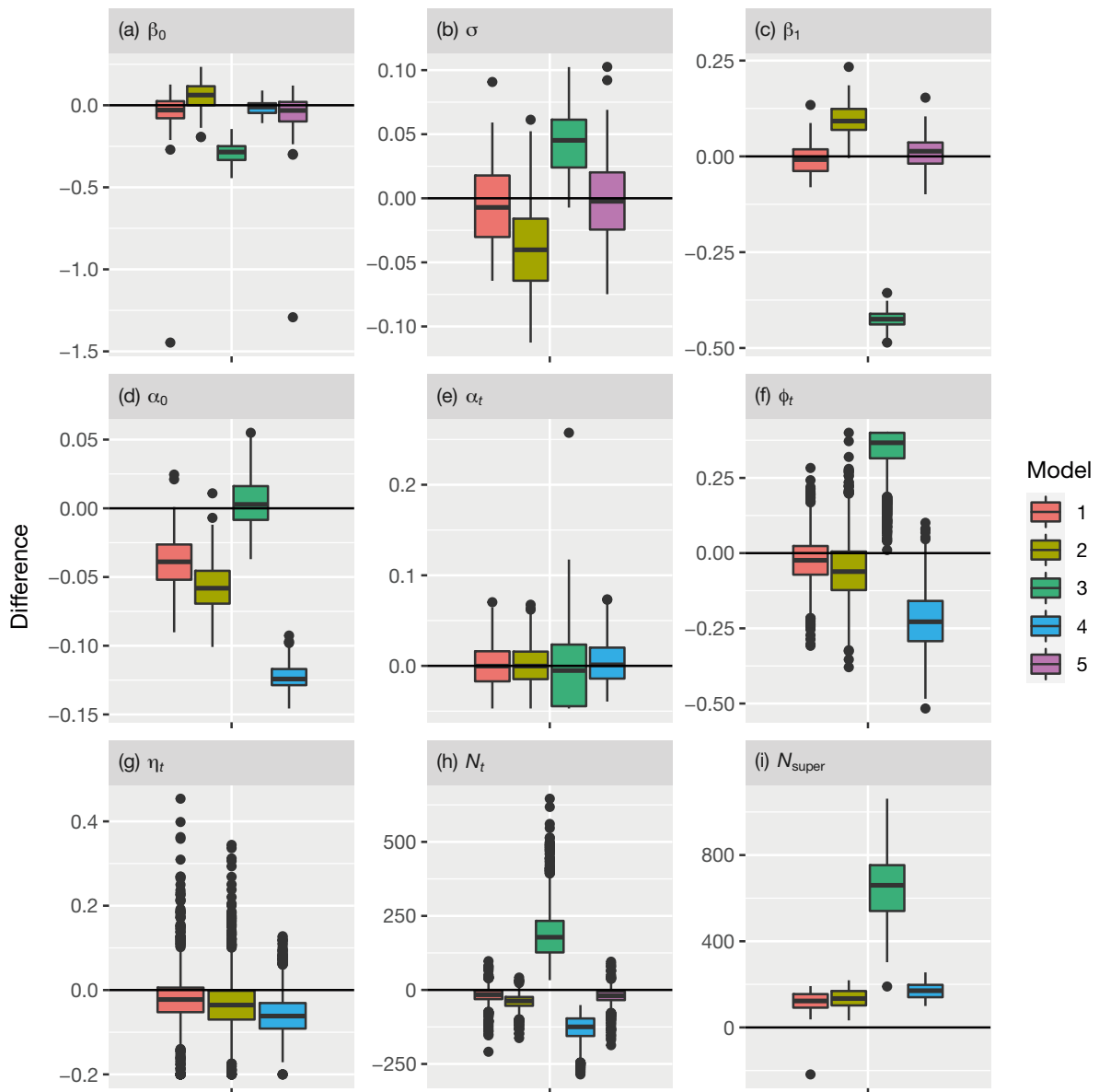


Fig. 5. Performance of 5 capture–recapture models applied to 100 data sets simulated using the distribution of monthly survey efforts off Cape Cod, Massachusetts. Model 1: a telemetry-integrated open spatial capture–recapture (SCR) model allowing for temporary emigration. Model 2: a standard (i.e. non-telemetry-integrated) version of the same model. Model 3: a standard open SCR model that did not allow for temporary emigration. Model 4: a non-spatial version of the model allowing for temporary emigration but that did not account for individual variation in space use or survey effort. Model 5: a closed SCR model that estimated  $N_t$  independently and did not account for movements between primary periods. For each boxplot, the thick black line in the middle: median difference between the estimated and true value; top of the box: first quartile; bottom of the box: third quartile; whisker bars: 1.5 times the interquartile range from the median; points: outliers. Individual panels (a–i) represent the estimated and derived parameters defined in Table 1 and described in the text. Note that not every parameter was estimated in every model as described in the text

season. The estimated baseline encounter rate ( $\beta_0 = -2.87; -3.09$  to  $-2.66$ ) translated into a relatively low baseline probability of encounter in each grid cell ( $p_0 = 0.05; 0.04$ – $0.07$ ) that increased with survey effort ( $\beta_1 = 0.30; 0.23$ – $0.38$ ). As expected, the estimated spatial scale parameter that described the

decline in encounter rate with distance from an individual's activity center was large ( $\sigma = 14.7$  km;  $13.5$ – $15.9$  km), reflecting the high mobility of the species.

Parameter estimates for the open component of the model varied among primary periods, suggesting that individuals did not enter and exit the surveyed

Table 2. Model selection summary for open spatial capture–recapture models applied to estimate the abundance of white sharks off Cape Cod, Massachusetts. Only parameters that varied during model selection are indicated here for ease of interpretation; the full model specification is provided in the text. The model selected to estimate abundance is indicated with **bold** text.  $k$ : number of parameters; nLL: negative log likelihood; AIC: Akaike information criterion;  $\Delta$ AIC: the difference in AIC relative to the best-fitting model;  $\beta_0$ : baseline encounter rate;  $\phi$ : probability an individual that was 'present' during a primary occasion remained in the surveyed area in the next;  $\eta$ : probability an individual that was previously part of the surveyed population but 'away' returned to the area between primary occasions

Model	$k$	nLL	AIC	$\Delta$ AIC
<i>Tagging effect</i>				
$\beta_0$ : year	81	2633	5427	359
$\phi$ : primary occasion + tagging				
$\eta$ : primary occasion + tagging				
$\beta_0$ : year	79	2684	5528	460
$\phi$ : primary occasion				
$\eta$ : primary occasion				
<i>Baseline encounter rate</i>				
$\beta_0$ : <b>constant</b>	<b>76</b>	<b>2458</b>	<b>5068</b>	<b>0</b>
$\phi$ : <b>primary occasion</b>				
$\eta$ : <b>primary occasion</b>				
<i>Probability of remaining and returning</i>				
$\beta_0$ : constant	51	2502	5106	38
$\phi$ : month				
$\eta$ : month				
$\beta_0$ : constant	43	2575	5236	168
$\phi$ : constant				
$\eta$ : constant				

population predictably (Table 3). However, across survey years, monthly estimates were generally indicative of northward migration into the region in the summer and a reverse southward migration in the fall. 'New' sharks entered the surveyed population throughout the monitoring period each year but were most likely to enter the surveyed population in July or August (Table 3). Although  $\phi_t$  varied substantially over time, once 'present', individual sharks were roughly equally likely to remain in the region between primary occasions ( $\bar{\phi} = 0.55$  for June through September) until October ( $\phi_t \leq 0.08$ ). Estimates of  $\phi_t$  were highest but most variable in July and August (Table 3), which was indicative of differing degrees of residency for sharks visiting the aggregation site over time. The probability that a shark that was present in October (and presumably migrated for the winter) had returned the subsequent June was low ( $\phi_t \leq 0.08$ ). This was likely reflective of inter-annual and inter-individual variation in migratory patterns, as was variation in the probabil-

ity that an individual that was previously part of the surveyed population returned to the area between primary occasions; there were no apparent trends in estimates of  $\eta_t$  across survey years (Table 3). The low probability of encounter resulted in a high degree of uncertainty in parameter estimates for several primary occasions (Table 3) that was also indicative of variation among individuals not accounted for by space use alone.

Monthly trends in abundance were also reflective of the species' seasonal migration into and out of the region (Table 3, Fig. 6). In all years, abundance was lowest at the beginning of the survey season (July in 2015 and June in 2016–2018) and increased during mid- to late summer (August or September). Monthly abundance decreased following the mid-season peak as individuals began to migrate south in all years other than 2017, when abundance decreased in September but increased again in October, perhaps as individuals that migrated further north returned to the area during their southward migration. While seasonal trends were generally similar among survey years, peak monthly abundance estimates increased over the survey period. We estimated a peak monthly population size of 190 individuals (95% CI = 144–237) in August 2015; 158 (110–206) in July 2016; 297 (229–365) in October 2017; and 519 (385–652) in September 2018. Based on the open and closed components of the model, we estimated 800 (393–1286) white sharks visited the Cape Cod aggregation site over the entire survey period. We note that the lower limit of the estimated 95% CI was 314 individuals, which extended below the number of individuals documented during the survey. Therefore, we increased the lower limit to the number of individuals encountered (Otis et al. 1978). This would imply that over half of the individuals in the  $N_{\text{super}}$  were present in September 2018, which seems unlikely.

When we compared the 2 goodness-of-fit statistics for the observed data set to the reference distributions from the simulated data sets, we found that the assumption of uniformly distributed activity centers and the fit of the observation model were adequate for most, but not all, primary occasions (Figs. S2 & S3). The value of  $FT_1$  for the observed data set fell within the distribution of the simulated data sets in all but 4 primary periods: September and October 2015 and September and October 2018, though it also fell near the extreme ends of the range in other occasions (Fig. S2). This suggests that the assumption of spatial randomness did not represent the observed data well in those months. Values of  $FT_2$  for the observed data set mostly fell within the distribu-



Table 3. Parameter estimates for each monthly primary sampling occasion from an open spatial capture–recapture model applied to estimate the abundance of white sharks off Cape Cod, Massachusetts; 95% CIs are indicated in parentheses; –: a parameter that was not estimated for that primary occasion. Parameters that did not vary by primary occasion (Table 1) are presented in the text; see Table 1 for definition of parameters. Gray shading distinguishes estimates corresponding to the different years of the survey

Occasion	Year-month	$N_t$	$\alpha_t$	$\phi_t$	$\eta_t$
1	2015-07	97 (54–139)	0.12 (0.07–0.17)	0.74 (0.47–1.00)	–
2	2015-08	190 (144–237)	0.15 (0.09–0.20)	0.36 (0.20–0.52)	0.07 (0.00–0.63)
3	2015-09	95 (56–133)	0.02 (0.00–0.05)	0.55 (0.25–0.85)	0.00 (0.00–0.00)
4	2015-10	109 (66–151)	0.06 (0.02–0.09)	0.00 (0.00–0.00)	0.08 (0.00–0.19)
5	2016-06	39 (12–66)	0.03 (0.00–0.06)	0.51 (0.00–1.00)	0.32 (0.18–0.47)
6	2016-07	158 (110–206)	0.07 (0.03–0.12)	0.43 (0.28–0.58)	0.15 (0.03–0.26)
7	2016-08	96 (68–123)	0.02 (0.00–0.04)	0.55 (0.37–0.74)	0.31 (0.18–0.43)
8	2016-09	157 (115–199)	0.05 (0.02–0.09)	0.65 (0.41–0.90)	0.06 (0.00–0.19)
9	2016-10	137 (90–184)	0.02 (0.00–0.05)	0.08 (0.00–0.20)	0.00 (0.00–0.00)
10	2017-06	25 (3–47)	0.02 (0.00–0.04)	0.24 (0.00–0.66)	0.19 (0.11–0.26)
11	2017-07	91 (61–121)	0.03 (0.00–0.06)	0.95 (0.71–1.00)	0.20 (0.10–0.30)
12	2017-08	204 (157–252)	0.10 (0.06–0.14)	0.46 (0.25–0.66)	0.12 (0.00–0.25)
13	2017-09	117 (75–159)	0.02 (0.00–0.06)	0.64 (0.33–0.95)	0.41 (0.25–0.57)
14	2017-10	297 (229–365)	0.06 (0.02–0.11)	0.00 (0.00–0.00)	0.07 (0.00–0.14)
15	2018-06	17 (3–30)	0.00 (0.00–0.01)	0.21 (0.00–0.60)	0.23 (0.16–0.30)
16	2018-07	160 (122–199)	0.10 (0.06–0.14)	0.55 (0.40–0.70)	0.29 (0.21–0.37)
17	2018-08	250 (200–299)	0.08 (0.04–0.12)	1.00 (1.00–1.00)	0.13 (0.00–0.31)
18	2018-09	519 (385–652)	0.04 (0.01–0.08)	0.47 (0.36–0.58)	0.19 (0.08–0.29)
19	2018-10	279 (215–343)	0.00 (0.00–0.00)	–	–

tion of simulated data sets except for 3 months in 2018 (July, August, and September; Fig. S3), indicating the observation model did not describe individual encounters in each grid cell ‘trap’ well in those periods, potentially resulting in biased estimates of abundance in those primary occasions.

#### 4. DISCUSSION

We have generated the first estimate of abundance for the white shark at a new seasonal aggregation site in the WNA, which required the development of a novel modeling framework to accommodate the species’ migratory behavior. The highly migratory habits of white sharks have complicated previous efforts to estimate abundance at seasonal aggregation sites (Burgess et al. 2014) but have been difficult to account for explicitly in conventional capture–recapture models given their lack of spatial context. In this study, we extended an existing open SCR model fit in a computationally efficient maximum likelihood framework (Glennie et al. 2019) to allow for movements into and out of the surveyed area and accommodate variation in residency and habitat use among individuals. Our simulation testing demonstrated that models failing to account for either movement-related source of heterogeneity produced biased estimates of abundance that would be mis-

leading if used as the basis for management advice. We applied the model to describe the seasonal dynamics of the white shark aggregation off Cape Cod from 2015–2018 and estimated an  $N_{\text{super}}$  size of 800 (393–1286) individuals. This represents the first estimate of abundance for the species in any portion of its WNA range and provides an important baseline from which the performance of current and future management measures can be assessed for this species of conservation concern. In addition, by directly linking changes in abundance over time to the demographic processes underpinning them (i.e. recruitment, emigration, immigration), our model provides a more mechanistic understanding of the dynamics of white shark aggregations, improving the applied relevance of the results for the conservation and management of the species.

By explicitly accounting for space, our open SCR model provides a biologically intuitive framework that is flexible enough to accommodate several sources of bias common to white shark capture–recapture surveys. In particular, we were able to account for 3 processes that influence individual encounter probabilities that have not been previously addressed in white shark photo-ID studies: (1) spatial variation in survey effort; (2) individual variation in habitat use; and (3) individual movements into and out of the surveyed area. Spatial variation in survey effort has received the least consideration in previous studies

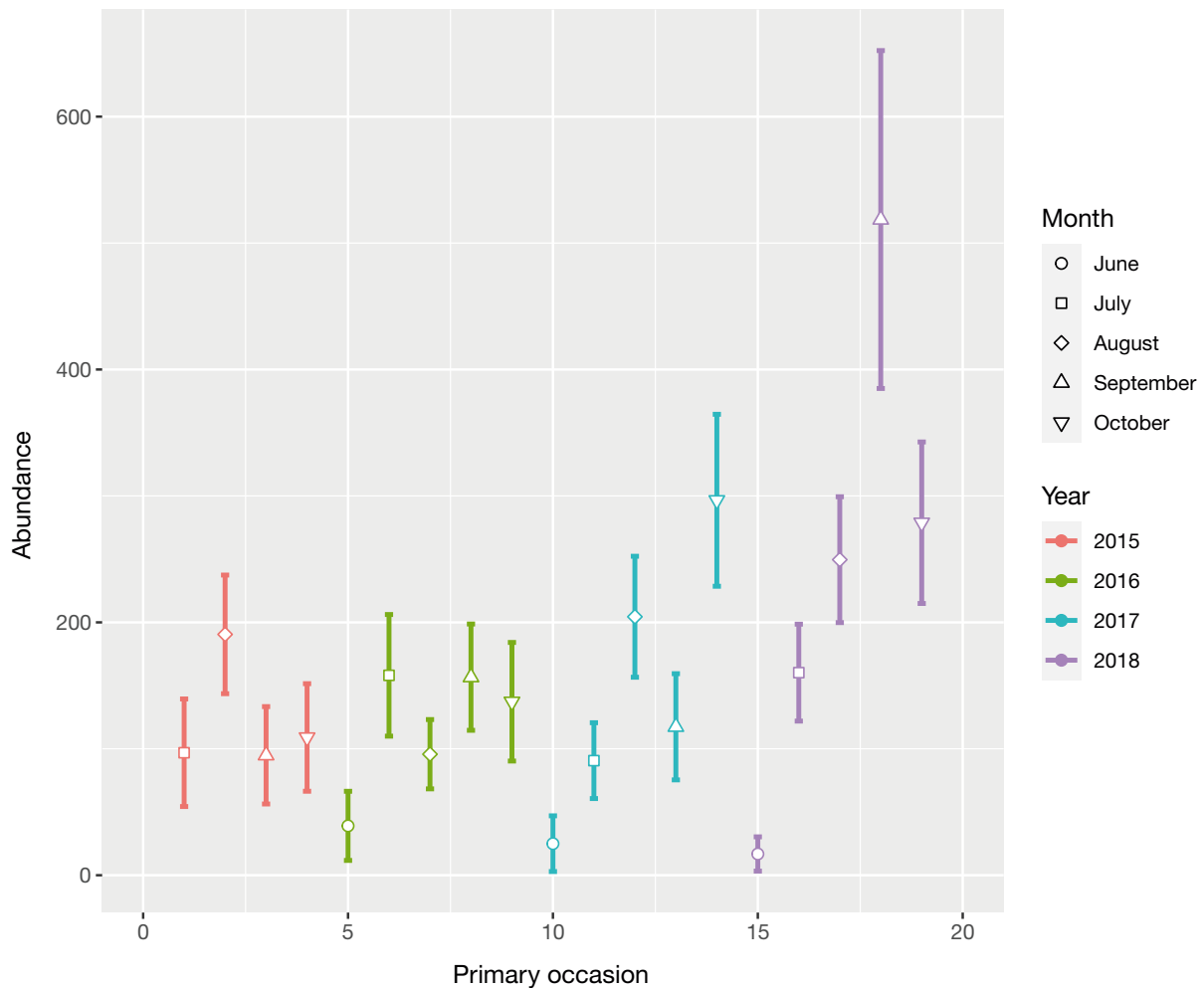


Fig. 6. Estimated abundance (points with 95% CIs) of white sharks off Cape Cod, Massachusetts, in each monthly primary occasion

of white shark aggregation sites, but the location and intensity of sampling effort influence an individual's probability of encounter in a fashion similar to other sources of heterogeneity (Otis et al. 1978, Royle et al. 2009, Thompson et al. 2012). Ideally, researchers would control for this source of bias by following systematic survey designs, but standardized surveys would be unlikely to generate sufficient encounters to yield reliable abundance estimates due to the species' mobility and dynamic habitat use at aggregation sites. Because of this, many white shark monitoring programs are unstructured or opportunistic in nature and, in several regions, primarily rely on encounters recorded by ecotourists (Domeier & Nasby-Lucas 2007, Towner et al. 2013). Provided some measure of effort is recorded, our modeling framework can be generalized to accommodate data collected opportunistically using static (e.g. cage diving sites; Domeier & Nasby-Lucas 2007) or mobile (e.g. boat-

based tours) unstructured approaches. Although additional simulation testing and alternative data collection scenarios should be further explored, our approach appears to perform well for unstructured surveys with variable sampling effort in space and time, even when individual encounter probabilities are low and the resulting uncertainty in the estimates is high.

Our findings reinforce the results of previous studies that have highlighted the importance of accounting for the movement ecology of the species when estimating white shark abundance from capture–recapture data (Burgess et al. 2014). Individual white sharks vary widely in their migratory behavior and use of aggregation sites (Jorgensen et al. 2010, Jewell et al. 2013, Kock et al. 2013, Francis et al. 2015, Hoyos-Padilla et al. 2016, Skomal et al. 2017, Winton et al. 2021); as our simulation testing demonstrated, this induces heterogeneity in encounter probabilities that non-spatial and closed capture–recapture mod-

els cannot accommodate. By adopting an open SCR approach, we were able to model individual heterogeneity related to habitat use, which likely subsumes many sources of variation previously considered for white sharks. However, as with any model, ours involves several simplifying assumptions. The implications and potential ramifications of violating the core assumptions in non-spatial capture–recapture models, including those related to movement, have been discussed in detail elsewhere (Otis et al. 1978, Burgess et al. 2014), as have those related to the functional relationships used to describe variation in encounter probabilities and space use in SCR models (Royle et al. 2013). Therefore, we do not discuss them further but comment on two potentially important sources of movement-related heterogeneity at white shark aggregation sites that our model does not account for here.

Standard SCR models, which we used to estimate abundance during primary periods, assume that individual activity centers are independent and uniformly distributed over the state space and that  $\sigma$  (which governs the decay in encounter probability with distance from an individual's center of activity and therefore reflects the scale of movement) is symmetric and constant among individuals and over the time step. This is almost certainly not the case for white sharks; individuals interact with conspecifics in agonistic (Domeier & Nasby-Lucas 2007) and possibly associative (Papastamatiou et al. 2022) ways, and larger, more dominant individuals typically patrol smaller areas and exhibit higher degrees of residency at aggregation sites than smaller individuals (Goldman & Anderson 1999, Jewell et al. 2013). In addition, the space use and distribution of white sharks at coastal sites varies in response to prey species and environmental conditions and are likely asymmetrically distributed along the coastline (Goldman & Anderson 1999, Brown et al. 2010, Kock et al. 2013, Hoyos-Padilla et al. 2016, Santana-Morales et al. 2021). These types of interactions were likely the cause of the relatively poor fit of the model applied to the Cape Cod aggregation in some time steps but would require additional data sources and further model development to address (Royle et al. 2013, Sutherland et al. 2015). Provided sufficient data were available (e.g. sex, stage, or class status available for every individual; remotely sensed environmental data at the appropriate resolution), both processes could be included in our model to answer questions related to the social and environmental dynamics of white shark aggregations (Russell et al. 2012, Royle et al. 2013, Reich & Gardner 2014, Sutherland et al. 2015,

McLaughlin & Bar 2021). However, this additional complexity may require the integration of other data types given the typically low number of individual recaptures achieved in white shark photo-ID studies.

Acoustic telemetry data can be directly incorporated into our model to inform abundance and demographic estimates. The relatively straightforward integration of georeferenced data sources, such as telemetry data, is an additional advantage of the spatial nature of our framework. Tagging studies are often conducted in conjunction with photo-ID surveys at aggregation sites (Delaney et al. 2012), and the data that are collected are used indirectly to aid in interpretation of the resulting abundance estimates and to assess the validity of model assumptions (Chapple et al. 2011, Burgess et al. 2014). Telemetry data have been directly integrated via additional likelihood components in closed SCR models for terrestrial carnivores to inform relationships with environmental covariates and the scale of the movement process via  $\sigma$  (Royle et al. 2013, Sollmann et al. 2013, Tenan et al. 2017, Linden et al. 2018) but have not previously been used to inform parameters related to movements into and out of the state space in an open SCR model. Our formulation allowed us to integrate 'known' states for almost 100 acoustically tagged individuals to jointly estimate probabilities of moving into and out of the state space from both data sources.

However, like all telemetry-integrated models developed to date, our model assumes that the movements and habitat use of tagged individuals can be considered representative of the broader population. This would require that individuals are randomly sampled from the population, which is difficult to achieve in any tagging study. Our results indicated inconsistency in the movement patterns of tagged and untagged white sharks, which is ultimately why we chose not to use the integrated model in our application to the Cape Cod aggregation site. In general, tagged individuals in our study had much higher encounter rates than expected given the distribution of all individuals encountered (Table S1, Fig. 4a), suggesting that tagged individuals exhibited a higher degree of fidelity to Cape Cod than is typical of the broader population. Because sharks that spend more time at aggregation sites are more available to tagging efforts (Hewitt et al. 2018), it seems likely that the subsample of tagged individuals at most sites is skewed towards more resident individuals. This makes applying telemetry-integrated approaches much more difficult than the simple addition of components to the likelihood and presents challenges beyond the scope of the work presented here (see

McClintock et al. 2022 for a review). We believe that the integration of telemetry data and more explicit models for movement into abundance estimates for white sharks is an exciting and important area of future research.

Applying our model to the encounter data collected along Cape Cod from 2015–2018, we generated monthly estimates of abundance and movements into and out of the surveyed area to characterize the seasonal dynamics of this new aggregation site. Consistent with previous tagging studies conducted in the region, we found that the number of sharks present peaks in the late summer and early fall as white sharks move into the waters along Cape Cod to feed on the locally abundant gray seal population (Skomal et al. 2012). While gray seals occur along Cape Cod year-round (Moxley et al. 2017), white sharks are seasonal visitors (Skomal et al. 2017), which supports the results of previous studies that suggest that water temperature limits their occurrence in the region (Curtis et al. 2014, Skomal et al. 2017).

Variation in month-specific abundance estimates across years likely reflects interannual variability in the suitability of thermal habitat but also suggests a possible increase in the annual abundance of white sharks over the course of the survey. Peak monthly estimates increased in each year of the survey, as did the number of individuals documented. This may indicate a true increase in the number of white sharks visiting the aggregation site over time but may also reflect better coverage of the northern extent of the Cape Cod coastline over the course of the survey (Fig. 2). White shark sightings were rarely reported along the northern stretch of the Cape Cod coastline prior to 2017 but became more common as the survey progressed. Whether this reflects distributional changes along Cape Cod as local densities increased or intensified sighting effort related to the growing shark ecotourism industry in the area is unclear. Regardless of the cause, because of the increase in sightings, considerably more survey effort was expended to the north in the last 2 yr of the survey. Though our model did account for variation in survey effort, persistent non-randomized sampling can lead to bias in abundance estimates, particularly if effort is concentrated in areas where densities are high (Russell et al. 2012, Moqanaki et al. 2021). The high estimated abundance for September 2018 (as well as the high persistence probability estimated for the previous month) may be indicative of this. Due to poor weather and water conditions, we were only able to conduct 3 surveys during that primary period, all of which were restricted to small stretches of the

coastline with high shark activity. Though there was no evidence of changes in baseline encounter rates over the course of the survey, it is also possible that the efficiency of our survey methods increased over time with experience, and that the same amount of effort in later years yielded more encounters than in early years of the survey. We assumed that the length of the research vessel's survey track provided a sufficient measure of effort as well as a cumulative proxy for environmental conditions impacting encounter rates. A more mechanistic understanding of how various factors influence survey encounter rates could be used to disentangle these types of effects in future studies. Despite our inability to fully resolve issues with model fit, we found that the observation model adequately described the observed data in most primary occasions, and it seems plausible the lack of fit that remains could be remediated if additional data sources were available. Therefore, we consider the abundance estimates presented here the best available given the existing data.

Our  $N_{\text{super}}$  estimate of 800 (393–1286) individuals for the 4 yr survey period is comparable to but larger than most previous estimates for other white shark aggregation sites near pinniped colonies conducted over similar time frames. Capture–recapture studies conducted over multiple years off South Africa (Cliff et al. 1996, Towner et al. 2013), central California (Chapple et al. 2011), South Australia (Strong et al. 1996), and Guadalupe Island, Mexico (Sosa-Nishizaki et al. 2012, Becerril-García et al. 2020), have estimated aggregation sizes from 78 to 1279 individuals. This suggests that Cape Cod is among the larger aggregation sites worldwide, especially considering that our estimate is likely an underestimate given our omission of 'potential' individuals (sharks that could not be matched to previously identified individuals but did not have the minimum number of features documented for inclusion in the analysis). Most sharks classified as 'potentials' were encountered less than 3 times (97%) and were likely transient individuals that did not spend much time in the waters along Cape Cod. Frameworks developed for such 'partial' identities could and should be used in future studies to account for this source of bias, but typically require Bayesian estimation approaches that can be computationally difficult to implement (McClintock et al. 2013, Augustine et al. 2018). The inability to fully document all individuals and account for known sources of heterogeneity in encounter probabilities is a persistent problem in white shark photo-ID studies (Burgess et al. 2014, Irion et al. 2017). As a result, all previous estimates

have been subject to similar but unquantifiable degrees of bias, complicating the comparison of estimates between sites. Even if variation among studies could be corrected for, earlier studies applied conventional capture–recapture models that required no clear definition of the area corresponding to abundance estimates. This means it is not straightforward to derive estimates of density at other sites, which would be a more informative metric for direct comparison than abundance (Royle et al. 2014).

We emphasize that our estimates only correspond to the individuals exposed to sampling during our survey along Cape Cod and are not representative of the entire WNA population. The Cape Cod aggregation site represents a small fraction of the species' overall range in the region (Curtis et al. 2014), and the extent of its importance to the broader population remains unclear. As is typical of white shark aggregations near pinniped colonies, the majority of the individuals we encountered were large juvenile and subadult white sharks, which reflects ontogenetic shifts in diet and habitat use (Francis et al. 2015). Young-of-the-year and small juvenile white sharks (<2.5 m TL) primarily feed on fish and small elasmobranchs (Hussey et al. 2012) and are more thermally restricted than larger individuals due to their smaller body mass (Curtis et al. 2014, Skomal et al. 2017, Shaw et al. 2021). During the summer and fall months when white shark activity off Cape Cod peaks, these size classes primarily occur south of the region in the New York Bight (Casey & Pratt 1985, Curtis et al. 2018, Shaw et al. 2021). As they grow larger and begin incorporating marine mammals into their diet (Hussey et al. 2012), white sharks are capable of migrating into cooler waters and undertake extensive migrations into more northern and offshore habitats to optimize foraging opportunities. Many of these larger individuals frequent areas near pinniped colonies, but not all individuals visit aggregation sites every year, if at all (Jorgensen et al. 2010, Skomal et al. 2017, Franks et al. 2021). Although their distribution is seasonally concentrated in the productive coastal waters along the northeastern USA and Canada, large juvenile, subadult, and adult white sharks are broadly dispersed along the entire Atlantic continental shelf during the summer and fall, with larger individuals, particularly mature females, regularly using offshore habitats (Skomal et al. 2017, Franks et al. 2021, Bowlby et al. 2022). If the proportion of the broader population visiting the waters off Cape Cod during the survey period was known, we could potentially account for the number of individuals 'available' to our survey to extrapolate

an estimate of overall population size. However, this would require stratified-random tagging and/or survey efforts throughout the species' range, which would be infeasible. While we recognize that the absolute size of the WNA population is likely far larger than that presented here (Burgess et al. 2014, Hillary et al. 2018), our results do provide a baseline estimate of abundance for the only known aggregation site in the region, where the species can be reliably encountered and monitored year after year.

Without historic abundance estimates, it is impossible to definitively determine if our estimates are indicative of population recovery, but the results of this and previous studies (Curtis et al. 2014) provide evidence that management measures implemented in the WNA in the 1990s have been effective. However, continued conservation concern seems reasonable given the species' inherent vulnerability to even low levels of mortality (Natanson & Skomal 2015, Bowlby & Gibson 2020). Current threats to the population have not been quantified, but white sharks observed off Cape Cod often bear evidence of interactions with fishing gear and boat strike wounds (M. V. Winton & G. B. Skomal unpubl. data). Therefore, even this relatively well-protected population may be experiencing substantial anthropogenic impacts. Continued monitoring of the aggregation could provide insights into the fitness implications and magnitude of these types of interactions and aid in the development of more targeted conservation strategies for the WNA population (Harvey-Carroll et al. 2021).

## 5. CONCLUSIONS

In one of the earliest studies describing the population dynamics of a white shark aggregation site, Strong et al. (1996, p. 401) stated '...there is clearly a need to develop a consistent means of assessing white shark population size.' Over 25 yr later, that need remains. A recent survey of 43 white shark scientists identified 'assessing the size and status of white shark populations' as the number one research priority for the species (Huveneers et al. 2018), but the white shark scientific community has yet to come to a consensus on how best to do so. Fierce debate surrounding two recent estimates (Chapple et al. 2011, Burgess et al. 2014, Andreotti et al. 2016, Irion et al. 2017) highlights the need for a more unified approach to enable regional comparisons, assess the performance of conservation measures for white sharks worldwide, and progress the field. We hope that the open SCR model developed here is a step towards

that goal. The hierarchical, spatial nature of our model provides a flexible framework that accounts for the movements of the species at aggregation sites and can be extended to intuitively account for other sources of bias (e.g. differences in the quantity or quality of baits or chum used to attract sharks to stationary sites, trap 'happiness' or 'shyness', dominance effects; Anderson et al. 2011, Chapple et al. 2011, Bruce & Bradford 2013, Towner et al. 2013). Importantly, the spatial aspect of the model provides a straightforward pathway for integrating other geo-referenced data sources, such as telemetry and standardized survey data, which could improve the robustness and extend the geographic scale of estimates beyond aggregation sites to tie local dynamics to those of the broader population. We recognize that approaches for assessing abundance throughout the species' range are needed (Hillary et al. 2018, Huveneers et al. 2018), but it seems likely that photo-ID surveys conducted at aggregation sites will remain the most logistically feasible approach for obtaining population data and the basis for monitoring white shark populations for the foreseeable future.

While it may seem counterintuitive, the need for reliable abundance estimates is more important than ever given that white shark populations in several regions, including the WNA, are seemingly recovering as a result of several decades of protection (Lowe et al. 2012, Curtis et al. 2014). As recovering populations return to regions where they have long been rare or absent, increased interactions between sharks and humans can create conflict and undermine public support of conservation policies (Ferretti et al. 2015, Carlson et al. 2019). Although the overall risk posed to recreational water users remains low even at aggregation sites (Ferretti et al. 2015), the sensational media coverage that typically accompanies white shark sightings and attacks on humans generates fear and can skew perceptions of risk (Neff & Hueter 2013). A lack of quantitative population information can heighten this sense of risk by raising doubt about the scientific basis for management decisions and eroding public trust (Artelle et al. 2018). Therefore, we view reliable abundance estimates as not only critical for management but also for navigating the complex societal conflicts that will arise when and where white shark populations recover, which will likely present the next major conservation challenge for this iconic species.

*Acknowledgements.* This study was funded in part by the Atlantic White Shark Conservancy, with additional funding provided by the state of Massachusetts. M.V.W. was par-

tially supported by a grant from MIT Sea Grant, Massachusetts Institute of Technology, pursuant to National Oceanic and Atmospheric Administration Award NA17OAR4170243. In particular, the authors thank Cynthia and Ben Wigren and Ken Johnson for their endless support and enthusiasm for this work. We also thank team members Captain John King and Pam King of the FV 'Aleutian Dream' and spotter pilot Wayne Davis. Special thanks to John Chisholm for beginning the ID work, to Chris Rillahan for developing the video processing algorithm, and to Samantha Weiss, Nathalie Staiger, Sam Luitjens, Victoria Migneco, Kelly Alves, Bella Horstmann, Sarah Feeley, and Ashleigh Novak for their efforts identifying sharks. Finally, we thank William Hoffman and Ben Gahagan (Massachusetts Division of Marine Fisheries; MADMF), who provided acoustic detection data from their receiver array and field support, and the many other acoustic array maintainers who contributed detection data via the Ocean Tracking Network and the Atlantic Cooperative Telemetry Network.

#### LITERATURE CITED

- Akaike H (1973) Information theory and an extension of the maximum likelihood principle. In: Petrov BN, Csàki BF (eds) Second international symposium on information theory. Akademiai Kiado, Budapest, p 267–281
- ✦ Anderson SD, Chapple TK, Jorgensen SJ, Klimley AP, Block BA (2011) Long-term individual identification and site fidelity of white sharks, *Carcharodon carcharias*, off California using dorsal fins. *Mar Biol* 158:1233–1237
- ✦ Andreotti S, Rutzen M, van der Walt S, Von der Heyden S and others (2016) An integrated mark–recapture and genetic approach to estimate the population size of white sharks in South Africa. *Mar Ecol Prog Ser* 552:241–253
- ✦ Artelle KA, Renolds JD, Treves A, Walsh JC, Paquet PC, Darimont CT (2018) Hallmarks of science missing from North American wildlife management. *Sci Adv* 4: eaao0167
- ✦ Augustine BC, Royle JA, Kelly MJ, Satter CB, Alonso RS, Boydston EE, Crooks KR (2018) Spatial capture–recapture with partial identity: an application to camera traps. *Ann Appl Stat* 12:67–95
- ✦ Becerril-García EE, Hoyos-Padilla EM, Santana-Morales O, Gutiérrez-Ortiz M, Ayala-Bocos A, Galván-Magaña F (2020) An estimate of the number of white sharks *Carcharodon carcharias* interacting with ecotourism in Guadalupe Island. *J Fish Biol* 97:1861–1864
- ✦ Borchers DL, Efford MG (2008) Spatially explicit maximum likelihood methods for capture–recapture studies. *Biometrics* 64:377–385
- ✦ Bowlby HD, Gibson AJF (2020) Implications of life history uncertainty when evaluating status in the Northwest Atlantic population of white shark (*Carcharodon carcharias*). *Ecol Evol* 10:4990–5000
- ✦ Bowlby HD, Benoît HP, Joyce W, Sulikowski J and others (2021) Beyond post-release mortality: inferences on recovery periods and natural mortality from electronic tagging data for discarded lamnid sharks. *Front Mar Sci* 8:619190
- ✦ Bowlby HD, Warren NJ, Winton MV, Coates PJ, Skomal GB (2022) Conservation implications of white shark (*Carcharodon carcharias*) behaviour at the northern extent of their range in the Northwest Atlantic. *Can J Fish Aquat Sci* 79:1843–1859

- Brown AC, Lee DE, Bradley RW, Anderson S (2010) Dynamics of white shark predation on pinnipeds in California: effects of prey abundance. *Copeia* 2010:232–238
- Bruce BD, Bradford RW (2012) Habitat use and spatial dynamics of juvenile white sharks, *Carcharodon carcharias*, in eastern Australia. In: Domeier ML (ed) Global perspectives on the biology and life history of the white shark. CRC Press, Boca Raton, FL, p 225–254
- Bruce BD, Bradford RW (2013) The effects of shark cagediving operations on the behavior and movements of white sharks, *Carcharodon carcharias*, at the Neptune Islands, South Australia. *Mar Biol* 160:889–907
- Burgess GH, Bruce BD, Cailliet GM, Goldman KJ and others (2014) A re-evaluation of the size of the white shark (*Carcharodon carcharias*) population off California, USA. *PLOS ONE* 9:e98078
- Carlson JK, Heupel MR, Young CN, Cramp JE, Simpfendorfer CA (2019) Are we ready for elasmobranch conservation success? *Environ Conserv* 46:264–266
- Casey JG, Pratt HL Jr (1985) Distribution of the white shark, *Carcharodon carcharias*, in the western North Atlantic. In: Sibley G, Seigel JA, Swift CC (eds) Biology of the white shark: a symposium. Memoirs of the Southern California Academy of Sciences, Vol 9. University of California at San Diego, San Diego, CA, p 2–14
- Castro JI (2012) A summary of observations on the maximum size attained by the white shark, *Carcharodon carcharias*. In: Domeier ML (ed) Global perspectives on the biology and life history of the white shark. CRC Press, Boca Raton, FL, p 85–90
- Chapple TK, Jorgensen SJ, Anderson SD, Kanive PE, Klimley AP, Botsford LW, Block BA (2011) A first estimate of white shark, *Carcharodon carcharias*, abundance off Central California. *Biol Lett* 7:581–583
- Chapple TK, Chambert T, Kanive PE, Jorgensen SJ and others (2016) A novel application of multi-event modeling to estimate class segregation in a highly migratory oceanic vertebrate. *Ecology* 97:3494–3502
- Cliff G, van der Elst RP, Govender A, Witthuhn TK, Bullen EM (1996) First estimates of mortality and population size of white sharks on the South African coast. In: Klimley AP, Ainley DG (eds) Great white sharks: the biology of *Carcharodon carcharias*. Academic Press, San Diego, CA, p 393–400
- Curtis TH, McCandless CT, Carlson JK, Skomal GB and others (2014) Season distribution and historic trends in abundance of white sharks, *Carcharodon carcharias*, in the western North Atlantic Ocean. *PLOS ONE* 9:e99240
- Curtis TH, Metzger G, Fischer C, McBride B and others (2018) First insights into the movements of young-of-the-year white sharks (*Carcharodon carcharias*) in the western North Atlantic Ocean. *Sci Rep* 8:10794
- Delaney DG, Johnson R, Bester M, Gennari E (2012) Accuracy of using visual identification of white sharks to estimate residency patterns. *PLOS ONE* 7:e34753
- Domeier ML, Nasby-Lucas N (2007) Annual re-sightings of photographically identified white sharks (*Carcharodon carcharias*) at an eastern Pacific aggregation site (Guadalupe Island, Mexico). *Mar Biol* 150:977–984
- Domeier ML, Nasby-Lucas N (2013) Two-year migration of adult female white sharks (*Carcharodon carcharias*) reveals widely separated nursery areas and conservation concerns. *Anim Biotelem* 1:2
- Dupont G, Royle JA, Nawaz MA, Sutherland C (2021) Optimal sampling design for spatial capture–recapture. *Ecology* 102:e03262
- Ferretti F, Jorgensen S, Chapple TK, De Leo G, Micheli F (2015) Reconciling predator conservation with public safety. *Front Ecol Environ* 13:412–417
- Francis MP, Duffy C, Lyon W (2015) Spatial and temporal habitat use by white sharks (*Carcharodon carcharias*) at an aggregation site in southern New Zealand. *Mar Freshw Res* 66:900–918
- Franks BR, Tyminski JP, Hussey NE, Braun CD and others (2021) Spatio-temporal variability in white shark (*Carcharodon carcharias*) movement ecology during residency and migration phases in the western North Atlantic. *Front Mar Sci* 8:744202
- Glennie R, Borchers DL, Murchie M, Harmsen BJ, Foster RJ (2019) Open population maximum likelihood spatial capture–recapture. *Biometrics* 75:1345–1355
- Goldman KJ, Anderson SD (1999) Space utilization and swimming depth of white sharks, *Carcharodon carcharias*, at the South Farallon Islands, central California. *Environ Biol Fishes* 56:351–364
- Gowen TA, Crum NJ, Roberts JJ (2021) An open spatial capture–recapture model for estimating density, movement, and population dynamics from line-transect surveys. *Ecol Evol* 11:7354–7365
- Gudger EW (1950) A boy attacked by a shark, July 25, 1936 in Buzzard's Bay, Massachusetts with notes on attacks by another shark along the New Jersey coast in 1916. *Am Midl Nat* 44:714–719
- Harvey-Carroll J, Stewart JD, Carroll D, Mohamed B and others (2021) The impact of injury on apparent survival of whale sharks (*Rhincodon typus*) in South Ari Atoll Marine Protected Area, Maldives. *Sci Rep* 11:937
- Hewitt AM, Kock AA, Booth AJ, Griffiths CL (2018) Trends in sightings and population structure of white sharks, *Carcharodon carcharias*, at Seal Island, False Bay, South Africa, and the emigration of subadult female sharks approaching maturity. *Environ Biol Fishes* 101:39–54
- Hillary RM, Bravington MV, Patterson TA, Grewe P and others (2018) Genetic relatedness reveals total population size of white sharks in eastern Australia and New Zealand. *Sci Rep* 8:2661
- Hoyos-Padilla EM, Klimley AP, Galván-Magaña F, Antoniou A (2016) Contrasts in the movements and habitat use of juvenile and adult white sharks (*Carcharodon carcharias*) at Guadalupe Island, Mexico. *Anim Biotelem* 4:14
- Hussey NE, McCann HM, Cliff G, Dudley SF, Wintner SP, Fisk AT (2012) Size-based analysis of diet and trophic position of the white shark (*Carcharodon carcharias*) in South African waters. In: Domeier ML (ed) Global perspectives on the biology and life history of the white shark. CRC Press, Boca Raton, FL, p 27–49
- Huvaneers C, Apps K, Becerril-García EE, Bruce B and others (2018) Future research directions on the 'elusive' white shark. *Front Mar Sci* 5:455
- Irion DT, Noble LR, Kock AA, Gennari E and others (2017) Pessimistic assessment of white shark population status in South Africa: comment on Andreotti et al. (2016). *Mar Ecol Prog Ser* 577:251–255
- Jewell OJD, Johnson RL, Gennari E, Bester MN (2013) Fine scale movements and activity areas of white sharks (*Carcharodon carcharias*) in Mossel Bay, South Africa. *Environ Biol Fishes* 96:881–894

- Jorgensen SJ, Reeb CA, Chapple TK, Anderson S and others (2010) Philopatry and migration of Pacific white sharks. *Proc R Soc B* 277:679–688
- ✦ Kanive PE, Rotella JJ, Chapple TK, Anderson SD, White TD, Block BA, Jorgensen SJ (2021) Estimates of regional annual abundance and population growth rates of white sharks off central California. *Biol Conserv* 257:109104
- Kendall WL, Nichols JD, Hines JE (1997) Estimating temporary emigration using capture–recapture data with Pollock's robust design. *Ecology* 78:563–578
- ✦ Kessel ST, Cooke SJ, Heupel MR, Hussey NE, Simpfendorfer CA, Vagle S, Fisk AT (2014) A review of detection range testing in aquatic passive acoustic telemetry studies. *Rev Fish Biol Fish* 24:199–218
- Klimley AP, Anderson SD (1996) Residency patterns of white sharks at the south Farallon Islands, California. In: Klimley AP, Ainley DG (eds) *Great white sharks: the biology of *Carcharodon carcharias**. Academic Press, San Diego, CA, p 365–374
- ✦ Kock A, O'Riain MJ, Mauff K, Meÿer M, Kotze D, Griffiths C (2013) Residency, habitat use and sexual segregation of white sharks, *Carcharodon carcharias* in False Bay, South Africa. *PLOS ONE* 8:e55048
- Kristensen K, Nielsen A, Berg CW, Skaug H, Bell BM (2016) TMB: automatic differentiation and Laplace approximation. *J Stat Softw* 70:1–21
- ✦ Linden DW, Sirén APK, Pekins PJ (2018) Integrating telemetry data into spatial capture–recapture modifies inferences on multi-scale resource selection. *Ecosphere* 9:e02203
- Lowe CG, Blasius ME, Jarvis ET, Mason TJ, Goodmanlowe GD, O'Sullivan JB (2012) Historic fishery interactions with white sharks in the Southern California Bight. In: Domeier ML (ed) *Global perspectives on the biology and life history of the white shark*. CRC Press, Boca Raton, FL, p 169–186
- ✦ McClintock BT, Conn PB, Alonso RS, Crooks KR (2013) Integrated modeling of bilateral photo-identification data in mark–recapture analyses. *Ecology* 94:1464–1471
- ✦ McClintock BT, Abrahams B, Chandler RB, Conn PB and others (2022) An integrated path for spatial capture–recapture and animal movement modeling. *Ecology* 103:e3473
- ✦ McLaughlin P, Bar H (2021) A spatial capture–recapture model with attractions between individuals. *Environmetrics* 32:e2653
- ✦ McPherson JM, Myers RA (2009) How to infer population trends in sparse data: examples with opportunistic sighting records for great white sharks. *Divers Distrib* 15:880–890
- ✦ Mollomo P (1998) The white shark in Maine and Canadian Atlantic waters. *North-East Nat* 5:207–214
- ✦ Moqanaki EM, Milleret C, Tourani M, Dupont P, Bischof R (2021) Consequences of ignoring variable and spatially autocorrelated detection probability in spatial capture–recapture. *Landsc Ecol* 36:2879–2895
- ✦ Moxley JH, Bogomolni A, Hammill MO, Moore KMT and others (2017) Google haul out: earth observation imagery and digital aerial surveys in coastal wildlife management and abundance estimation. *Bioscience* 67:760–768
- Nasby-Lucas N, Domeier ML (2012) Use of photo identification to describe a white shark aggregation at Guadalupe Island, Mexico. In: Domeier ML (ed) *Global perspectives on the biology and life history of the white shark*. CRC Press, Boca Raton, FL, p 381–392
- ✦ Natanson LJ, Skomal GB (2015) Age and growth of the white shark, *Carcharodon carcharias*, in the western North Atlantic Ocean. *Mar Freshw Res* 66:387–398
- ✦ Neff C, Hueter R (2013) Science, policy, and the public discourse of shark 'attack': a proposal for reclassifying human–shark interactions. *J Environ Stud Sci* 3:65–73
- Otis DL, Burnham KP, White GC, Anderson DR (1978) Statistical inference from capture data on closed animal populations. *Wildl Monogr* 62:3–135
- ✦ Papastamatiou YP, Mourier J, TinHan T, Luongo S, Hosoki S, Santana-Morales O, Hoyos-Padilla M (2022) Social dynamics and individual hunting tactics of white sharks revealed by biologging. *Biol Lett* 18:20210599
- ✦ Pebesma E (2018) Simple features for R: standardized support for spatial vector data. *R J* 10:439–446
- Pincock DG (2012) False detections: what are they and how to remove them from detection data. Application Note No. DOC-004691-03. Vemco, Halifax
- Plesnik E (2015) analyzeGPS: basic analysis of GPS data. R package version 0.1. <https://github.com/ehrscape/R-project/tree/master/AnalyzeGPS>
- ✦ Pollock KH (1982) A capture–recapture design robust to unequal probability of capture. *J Wildl Manag* 46:752–757
- R Core Team (2020) R: a language and environment for statistical computing. R Foundation for Statistical Computing, Vienna
- ✦ Reich BJ, Gardner B (2014) A spatial capture–recapture model for territorial species. *Environmetrics* 25:630–637
- ✦ Reid DD, Robbins WD, Peddemors VM (2011) Decadal trends in shark catches and effort from the New South Wales, Australia, shark meshing program 1950–2010. *Mar Freshw Res* 62:676–693
- ✦ Roff G, Brown CJ, Priest MA, Mumby PJ (2018) Decline of coastal apex shark populations over the past half century. *Commun Biol* 1:223
- ✦ Royle JA, Nichols JD, Ullas Karanth K, Gopalaswamy AM (2009) A hierarchical model for estimating density in camera-trap studies. *J Appl Ecol* 46:118–127
- ✦ Royle JA, Chandler RB, Sun CC, Fuller AK (2013) Integrating resource selection information with spatial capture–recapture. *Methods Ecol Evol* 4:520–530
- Royle JA, Chandler RB, Sollmann R, Gardner B (2014) *Spatial capture–recapture*. Academic Press, Waltham, MA
- ✦ Royle JA, Fuller AK, Sutherland C (2016) Spatial capture–recapture models allowing Markovian transience or dispersal. *Popul Ecol* 58:53–62
- ✦ Russell RE, Royle JA, Desimone R, Schwartz MK, Edwards VL, Pilgrim KP, McKelvey KS (2012) Estimating the abundance of mountain lions from unstructured spatial sampling. *J Wildl Manag* 76:1551–1561
- ✦ Santana-Morales O, Zertuche-Chanes R, Hoyos-Padilla EM, Sepúveda C and others (2021) An exploration of the population characteristics and behaviors of the white shark in Guadalupe Island, Mexico (2014–2019): observational data from cage diving vessels. *Aquat Conserv* 31:3480–3491
- ✦ Schwarz CJ, Arnason AN (1996) A general methodology for the analysis of capture–recapture experiments in open populations. *Biometrics* 52:860–873
- ✦ Shaw RL, Cutris TH, Metzger G, McCallister MP, Newtown A, Fischer GC, Ajemian MJ (2021) Three-dimensional movements and habitat selection of young white sharks (*Carcharodon carcharias*) across a temperate continental shelf ecosystem. *Front Mar Sci* 8:643831



- ✦ Sippel T, Eveson JP, Galuardi B, Lam C and others (2015) Using movement data from electronic tags in fisheries stock assessment: a review of models, technology and experimental design. *Fish Res* 163:152–160
- Skomal GB, Chisholm J, Correia SJ (2012) Implications of increasing pinniped populations on the diet and abundance of white sharks off the coast of Massachusetts. In: Domeier ML (ed) *Global perspectives on the biology and life history of the white shark*. CRC Press, Boca Raton, FL, p 405–417
- ✦ Skomal GB, Braun CD, Chisholm JH, Thorrold SR (2017) Movements of the white shark *Carcharodon carcharias* in the North Atlantic Ocean. *Mar Ecol Prog Ser* 580:1–16
- ✦ Sollmann R, Gardner B, Parsons AW, Stocking JJ and others (2013) A spatial mark–resight model augmented with telemetry data. *Ecology* 94:553–559
- Sosa-Nishizaki O, Morales-Bojórquez E, Nasby-Lucas N, Oñate-González E, Domeier ML (2012) Problems with photo identification as a method of estimating abundance of white sharks, *Carcharodon carcharias*. In: Domeier ML (ed) *Global perspectives on the biology and life history of the white shark*. CRC Press, Boca Raton, FL, p 393–404
- Strong WR Jr, Bruce BD, Nelson DR, Murphy RD (1996) Population dynamics of white sharks in Spencer Gulf, South Australia. In: Klimley AP, Ainley DG (eds) *Great white sharks: the biology of *Carcharodon carcharias**. Academic Press, San Diego, CA, p 401–414
- ✦ Sutherland C, Fuller AK, Royle JA (2015) Modelling non-Euclidean movement and landscape connectivity in highly structured ecological networks. *Methods Ecol Evol* 6:169–177
- ✦ Tenan S, Pedrini P, Bragalanti N, Groff C, Sutherland C (2017) Data integration for inference about spatial processes: a model-based approach to test and account for data inconsistency. *PLOS ONE* 12:e0185588
- ✦ Thompson CM, Royle JA, Garner JD (2012) A framework for inference about carnivore density from unstructured spatial sampling of scat using detector dogs. *J Wildl Manag* 76:863–871
- ✦ Towner AV, Wcisel MA, Reisinger RR, Edwards D, Jewell OJD (2013) Gauging the threat: the first population estimate for white sharks in South Africa using photo identification and automated software. *PLOS ONE* 8: e66035
- ✦ Winton MV, Sulikowski J, Skomal GB (2021) Fine-scale vertical habitat use of white sharks at an emerging aggregation site and implications for public safety. *Wildl Res* 48: 345–360
- Zucchini W, MacDonald IL (2009) *Hidden Markov models for time series: an introduction using R*. Chapman & Hall/CRC Press, Boca Raton, FL

*Editorial responsibility: Myron Peck,  
Den Burg, The Netherlands  
Reviewed by: 3 anonymous referees*

*Submitted: March 28, 2023  
Accepted: June 30, 2023  
Proofs received from author(s): July 24, 2023*